- 1 BREAKTHROUGH REPORT
- 2 Altering cold-regulated gene expression decouples the salicylic acid-growth
- 3 trade-off in Arabidopsis

- 5 María A. Ortega^{1,2,3}†, Rhodesia M. Celoy^{1,2}†, Francisco Chacon^{1,2}†, Yinan Yuan⁴, Liang-
- Jiao Xue^{1,2,5}, Saurabh P. Pandey^{1,2,3}, MaKenzie R. Drowns^{1,2,3}, Brian H. Kvitko⁶, Chung-Jui
- 7 Tsai^{1,2,3}*

8

- ¹Warnell School of Forestry and Natural Resources, University of Georgia; Athens, GA, USA.
- ²Department of Genetics, University of Georgia; Athens, GA, USA
- ³Department of Plant Biology, University of Georgia; Athens, GA, USA.
- ⁴College of Forest Resources and Environmental Science, Michigan Technological University;
- 13 Houghton, MI, USA
- ⁵State Key Laboratory of Tree Genetics and Breeding, College of Forestry, Nanjing Forestry
- 15 University; Nanjing, Jiangsu, China
- ⁶Department of Plant Pathology, University of Georgia; Athens, GA, USA.
- †Present address: M.A.O., Inari Agriculture, Ghent, Belgium; R.M.C., Agriculture and Agri-
- Food Canada, Lethbridge Research and Development Center, Lethbridge, Alberta, Canada; F.C.,
- Huck Institutes of the Life Sciences, Pennsylvania State University, University Park, PA, USA.

20

- 21 Keywords: Growth–defense trade-off, sub-ambient temperatures, salicylic acid, membrane
- 22 protection, phytohormone

23

24 **Short title:** Decoupling of growth–defense trade-offs

25

26

27

2829

*Corresponding author: Chung-Jui Tsai (cjtsai@uga.edu)

30	
31	The author responsible for distribution of materials integral to the findings presented in this
32	article in accordance with the policy described in the Instructions for Authors
33	(https://academic.oup.com/plcell/pages/General-Instructions) is: Chung-Jui Tsai
34	(cjtsai@uga.edu).
35	
36	Abstract
37	
38	In Arabidopsis (Arabidopsis thaliana), overproduction of salicylic acid (SA) increases disease
39	resistance and abiotic stress tolerance but penalizes growth. This growth-defense trade-off has
40	hindered the adoption of SA-based disease management strategies in agriculture. However,
41	investigation of how SA inhibits plant growth has been challenging because many SA-
42	hyperaccumulating Arabidopsis mutants have developmental defects due to the pleiotropic
43	effects of the underlying genes. Here, we heterologously expressed a bacterial SA synthase gene
44	in Arabidopsis and observed that elevated SA levels decreased plant growth and reduced the
45	expression of cold-regulated (COR) genes in a dose-dependent manner. Growth suppression was
46	exacerbated at below-ambient temperatures. Severing the SA-responsiveness of individual COR
47	genes was sufficient to overcome the growth inhibition caused by elevated SA at ambient and
48	below-ambient temperatures while preserving disease- and abiotic-stress-related benefits. Our
49	results show the potential of decoupling SA-mediated growth and defense trade-offs for
50	improving crop productivity.
51	
52	
53	

Introduction

5455

The phytohormone salicylic acid (SA) has well-established roles in immune signaling in plants 56 (Vlot et al., 2009; Peng et al., 2021; Ullah et al., 2023). Considerable advances in understanding 57 SA-mediated defense mechanisms have been made possible through forward genetic screens, 58 particularly in the model plant Arabidopsis (Arabidopsis thaliana). These screens have identified 59 mutants with enhanced disease resistance resulting from increased SA accumulation (Heil and 60 Baldwin, 2002; Rivas-San Vicente and Plasencia, 2011). Examples include constitutive 61 expresser of pathogenesis-related genes5 (cpr5) (Bowling et al., 1997), defense no death1 62 (dnd1) (Yu et al., 1998), sap and miz1 domain-containing ligase1 (siz1) (Lee et al., 2007), and 63 suppressor of rps4-RLD1 (srfr1) (Kwon et al., 2004). However, SA-elevated mutants exhibit 64 reduced growth, sometimes in a temperature-dependent manner (Heidel et al., 2004; Wang et al., 65 2009; Alcázar and Parker, 2011; Huot et al., 2014; Albrecht and Argueso, 2017). 66

67

68

69

70

71

72

73

74

75

76

77

78 79

80

81

82

83

84

Mechanistic research into the growth–defense trade-off has been challenging, in part because SA regulates various physiological and developmental processes in its own right (Rivas-San Vicente and Plasencia, 2011; Peng et al., 2021). Such efforts are further complicated by the reliance on the so-called autoimmune or lesion mimic mutants which display constitutive activation of defense responses (including elevated SA) at the expense of plant growth and development (Bruggeman et al., 2015; van Wersch et al., 2016). These autoimmune mutants have diverse origins, as their mutated genes are involved in not only immune signaling but also programmed or induced cell death, second messengers, hormonal pathways, or other cellular and subcellular processes (Bruggeman et al., 2015; van Wersch et al., 2016; Freh et al., 2022). This makes it difficult to isolate the specific effects of SA on growth. For instance, cpr5 mutants exhibit juvenile leaf senescence in additional to dwarfism (Bowling et al., 1997) and CPR5 was later shown to have dual function as a nucleoporin associated with the nuclear pore complex (Gu et al. 2016) and an RNA-binding protein associated with RNA processing complexes (Peng et al., 2022). The *dnd1* mutant shows severe dwarfism and harbors a loss-of-function allele encoding CYCLIC NUCLEOTIDE-GATED CATION CHANNEL2 (CNGC2) with roles in Ca²⁺ signaling associated with not only defense but also plant development (Köhler et al., 1999; Clough et al., 2000; Chan et al., 2003; Ma et al., 2010). SIZ1 encodes a small ubiquitin-like modifier (SUMO)

E3 ligase and its mutant phenotypes include altered chloroplast functions and prolific bolting (Miura et al., 2013; Kong et al., 2017). *SRFR1* encodes a tetratricopeptide repeat domain-containing protein that functions as a negative immune regulator via its interactions with disease resistance proteins as well as transcription factors involved in developmental processes (Kim et al., 2010; Li et al., 2010; Bhattacharjee et al., 2011; Kim et al., 2014). Disentangling the complex interplay between growth and SA-mediated defense calls for development of an experimental system to directly manipulate SA biosynthesis in plants without the confounding influence of pleiotropic gene mutations.

Several approaches have been used to augment SA biosynthesis in plants with varying degrees of success. In tobacco (Nicotiana tabacum), constitutive co-expression of Escherichia coli entC and Pseudomonas fluorescens pmsB genes encoding isochorismate synthase (ICS) and isochorismate pyruvate lyase (IPL), respectively, resulted in elevated SA accumulation and enhanced disease resistance when the enzymes were targeted to the chloroplasts (Verberne et al., 2000). However, a similar approach in Arabidopsis expressing a chloroplast-targeted fusion gene of pchA (ICS) and pchB (IPL) from Pseudomonas aeruginosa led to severe dwarfism and sterility (Mauch et al., 2001). This has discouraged further research with SA bioengineering in Arabidopsis. In poplars (Populus tremula × P. alba and P. nigra), SA hyperaccumulation resulting from overexpression of Yersinia enterocolitica Irp9 encoding a bifunctional SA synthase targeted to the chloroplasts enhanced abiotic stress tolerance and rust resistance without affecting plant growth as in tobacco (Xue et al., 2013; Ullah et al., 2022). The inconsistent results in Arabidopsis may reflect taxon-specific sensitivity to SA, although many autoimmune mutants with similar SA increases did not exhibit the same phenotypic severity or sterility (Bowling et al., 1997; Clough et al., 2000; Mauch et al., 2001; Lee et al., 2007; Kim et al., 2010). Alternatively, other experimental variations might have contributed, which justifies an independent reexamination.

In this study, we sought to augment plastidial SA biosynthesis in Arabidopsis by adopting the poplar strategy expressing a bacterial bifunctional SA synthase *Irp9* (Xue et al., 2013). We successfully obtained viable transgenic lines with a broad range of SA levels to directly assess the effects of SA on growth. We then used these lines to identify an inhibitory role of SA on

COLD-REGULATED (COR) gene expression. This SA inhibition interfered with multiple COR-associated functions, including leaf longevity and low temperature responses, which culminated in reduced growth especially at below-ambient temperatures. We provide evidence to suggest that the SA-mediated trade-off can be circumvented by transcriptional rewiring of CORs to balance growth and defense.

120121

116

117

118

119

122

123

Results

124

126

127

128

129

130

131

132

133

134

135

136

137

138

139

140

141

125 Elevated SA in transgenic Arabidopsis reduces growth in a dose dependent manner

We generated transgenic Arabidopsis plants overexpressing Irp9, a bacterial bifunctional SA synthase gene, with a ferredoxin chloroplast-targeting signal (Xue et al., 2013), named here Fd-Irp9-OE lines. We selected five independent lines with different levels of SA accumulation and growth phenotypes for characterization (Fig. 1). The SA-deficient transgenic NahG plants expressing a bacterial SA hydroxylase (Reuber et al., 1998) was included as reference. Four Fd-Irp9-OE lines (F24, F31, F36, and F51) had SA-derivative levels that approached or surpassed those detected in the autoimmune mutants, whereas line F19 was similar to the Col-0 wild type (WT) (Fig. 1A-C, Fig. S1). Hereafter, we refer to F24, F31, F36, and F51 as high-SA (hiSA) lines. The SA-related metabolites we detected are similar to those reported to increase in senescing or pathogen-challenged Arabidopsis leaves, or in mutants or natural accessions with elevated SA (Bartsch et al., 2010; Li et al., 2014) (Fig. S2). SA-glucoside (SAG) and dihydroxybenzoate xylosides (2,3-DHBX and 2,5-DHBX) were by far the most abundant SAderivatives in the hiSA lines, followed by dihydroxybenzoate glucosides (2,3-DHBG and 2,5-DHBG), with SA-glucose ester (SGE) detected at low levels (Fig. 1C, Fig. S1). For simplicity, we refer to these SA-derived compounds as SA metabolites, and their summed abundance as total SA levels.

142143

144

145

146

The increased accumulation of SA metabolites negatively affected hiSA plant growth in a dose-dependent manner under long-day (16 h light) conditions at 22°C (Fig. 1B–D). In the hiSA lines, we did not observe the developmental abnormalities associated with autoimmune mutants, such as prolific bolting (*siz1-2*), severe dwarfism (*dnd1*), or juvenile senescence (*cpr5-2*) (Fig. 1B and

inset). At 28 days after germination (DAG) of homozygous Fd-Irp9-OE lines, multiple growth parameters, including rosette size (length and thickness), rosette biomass, lateral root number, and root biomass were all inversely associated with total SA levels (Fig. 1D). Line F51 was the most severely affected, followed in order by F36, F31, and F24; F19 was phenotypically indistinguishable from the WT. The hiSA lines reached the reproductive phase (bolting) 4–6 days earlier than the WT and displayed accelerated senescence, with apparent leaf yellowing occurring 5–10 days before that in the WT (Fig. 1E–G). Accordingly, hiSA plants had shorter life spans and lower seed yields due to many undeveloped siliques as well as slightly reduced seed weight (Fig. 1F–H), although their fully developed seeds appeared normal (Fig. 1I). These results demonstrate an inhibitory effect of SA on growth and support previous findings on the role of SA in leaf senescence and seed yield (Morris et al., 2000; Abreu and Munné-Bosch, 2009; Zhang et al., 2013).

158 159

160

163

164

165

166

147

148

149

150

151

152

153

154

155

156

157

Transgenic hiSA plants exhibit enhanced disease resistance and abiotic stress tolerance

We assessed resistance to Pseudomonas syringae pv. tomato strain DC3000 (Pst DC3000) by 161 162

both syringe-infiltration of soil-grown plants and flood-inoculation of *in-vitro*-cultured seedlings

(F51 was excluded because of low seed yield) (Fig. 2). We observed a negative association

between leaf SA levels and bacterial growth three days post-inoculation (DPI), with significantly

lower bacterial growth in hiSA lines (Fig. 2A-B). These resistant lines showed mild disease

symptoms and continued to produce rosette leaves under the in vitro assay conditions, whereas

WT, F19, and *NahG* lines succumbed to *Pst* DC3000 during the monitoring period (Fig. 2B). 167

168

169

170

171

172

173

174

175

176

177

We also examined seedling sensitivity to abiotic stress treatments in vitro. Untreated F24, F31, and F36 seedlings had significantly shorter primary roots than the WT (Fig. 2C), consistent with the reduced root biomass of soil-grown plants (Fig. 1D). However, the reverse was true for seedlings grown on salt- or mannitol-containing medium (Fig. 2C). When seeds were sown on medium containing herbicidal methyl viologen, all four Fd-Irp9-OE lines, including F19, showed significantly higher germination rates than the WT (Fig. 2D). We noted that this SAmediated protection against methyl viologen-induced oxidative stress was partially lost in siz1-2 (Fig. 2D), highlighting the pleiotropic effects of the siz1 mutation (Kim et al., 2021). Taken together, our results demonstrate a functional dichotomy for elevated SA biosynthesis in

Arabidopsis; SA imposed a growth penalty under normal conditions but enhanced disease resistance and abiotic stress tolerance under adverse conditions.

181 Transgenic hiSA plants show constitutive expression of SAR marker genes but repression of COR

182 genes under nonstress conditions

We compared rosette transcriptomes of WT and Fd-Irp9-OE plants at bolting (stage 5.1, Boyes et al., 2001) under standard growth chamber conditions. The transcriptional response corresponded positively with SA levels, with 984, 890, 651, and 182 differentially expressed genes (DEGs, relative to WT) in F51, F36, F31, and F24, respectively, and none in F19 (Dataset S1). We detected 1825 DEGs in the SA-deficient NahG line. The two plants with the highest numbers of DEGs, F51 and NahG, shared 471 DEGs. Hierarchical clustering analysis of these 471 DEGs across all genotypes identified two main gene clusters with either SA-induced or SA-repressed expression (Fig. 3 and Dataset S1). Genes positively regulated by SA were enriched for the gene ontology (GO) terms 'systemic acquired resistance (SAR)' and 'response to SA' and various defense and signaling pathways (Fig. 3A-B), as would be predicted given the key function of SA in defense signaling. Examples of genes positively regulated by SA include the known SA markers *PATHOGENESIS-RELATED1* (PR1), PR2, and PR5 (Uknes et al., 1992) and WRKY transcription factor genes implicated in SAR (Wang et al., 2006).

Interestingly, the transcriptional responses differed within the *NONEXPRESSOR OF PR1* (*NPR*) family encoding SA receptors. *NPR3* and *NPR4*, but not *NPR1*, were induced in hiSA lines (Fig. 3A), which presumably reflects their distinct roles in SA signaling (Ding et al., 2018; Tran et al., 2023). Expression of pattern-triggered immunity (PTI) and effector-triggered immunity (ETI) marker genes (Yuan et al., 2021) was unaffected in hiSA lines (Dataset S1), except *FLS2* (*FLAGELLIN-SENSITIVE2*) and *CERK1* (*CHITIN ELICITOR RECEPTOR KINASE1*) which were significantly changed only in the extreme (*NahG*, F36, and F51) genotypes (Fig 3A, Dataset S1). Also unaffected was the expression of endogenous SA biosynthesis genes or their upstream regulators (Peng et al., 2021) (Dataset S1), but *SARD1* (*SAR DEFICIENT1*) was upregulated by SA (Fig. 3A). *S3H* and *S5H*, which encode SA 3-hydroxylase and SA 5-hydroxylase for SA catabolism into 2,3-DHBA and 2,5-DHBA, respectively (Fig. 1A) (Zhang et al., 2013; Zhang et al., 2017), were upregulated in an SA dose-dependent manner (Fig.

3A). The results are consistent with increased accumulation of 2,3-DHBA and 2,5-DHBA conjugates in hiSA leaves (Fig. 1C).

210

The smaller cluster of genes negatively regulated by SA showed significant GO enrichment for 211 'cold acclimation' and 'response to water deprivation' (Fig. 3B). In particular, members of four 212 COLD-REGULATED (COR) gene families [COR15, COR6.6 (KIN), COR47 (RD17 and 213 214 ERD10), COR78 (RD29) and their tandem duplicates, except when below detection known to be induced by cold (Thomashow, 1999) were downregulated in the hiSA lines (Fig. 3A). COR 215 genes are regulated by C-REPEAT/DEHYDRATION RESPONSIVE ELEMENT-BINDING 216 FACTORS (CBFs/DREBs) and INDUCERS OF CBF EXPRESSION (ICEs) best characterized 217 for their roles in freezing tolerance (Thomashow, 1999; Kim et al. 2015; Tang et al., 2020; Li et 218 al., 2024). ICE expression was low under nonstress conditions and unchanged in the hiSA lines. 219 220 Among the CBFs, we detected only CBF3 (DREB1A) transcripts, whose levels corresponded 221 negatively with SA like COR genes (Fig. 3A), supporting sub-functionalization of CBF members (Novillo et al., 2007). Together, these results confirm canonical SA responses in hiSA leaves 222 while also uncovering a negative effect of SA on COR gene expression. 223

- 225 SA-mediated growth penalty is exacerbated at below-ambient temperatures
- Motivated by the widespread downregulation of COR genes in the hiSA lines and by our 226 anecdotal observations of greater growth penalties during winter when plants were watered with 227 cold tap water, we conducted a series of temperature experiments to characterize the effects of 228 SA on growth in more detail. We first compared F24 with WT and NahG plants under different 229 temperature regimes (Fig. 4). Plant growth decreased as expected in all three genotypes as the 230 temperature decreased from 26°C to 16°C, but the penalty was most pronounced in F24 (Fig. 231 4A). When we compared multiple hiSA lines at 22°C and 16°C, their growth reduction was 232 exacerbated at below-ambient temperature in an SA-dose-dependent manner (Fig. 4B,C and Fig. 233 S3). Plants grown at 16°C showed significantly greater ion leakage than those at 22°C, and the 234 differences corresponded positively with SA levels (Fig. 4D). Elevated ion leakage resulting 235 from decreased membrane permeability is associated with chilling-induced injury and growth 236

reduction (Lyons, 1973). The data thus hint at a temperature-sensitive link between SA, membrane integrity, and plant growth.

239

240

241

242

243

244

245

246

247

248

249

250

251

252

253

254

We performed transcriptome analysis using rosette leaves of F24, WT, and NahG plants (stage 5.1) grown at 22°C:18°C (day:night, hereafter denoted as 22°C) or 18°C:16°C (day:night, hereafter 18°C) under otherwise identical long-day growth chamber conditions. We were particularly interested in genes responsive to SA perturbation at 18°C (F24 vs. WT and NahG vs. WT) and to cool temperatures (18°C vs. 22°C) in the WT. The intersection of the three DEG lists (118 genes) showed two major groups (Fig. 4E and Dataset S2). The first group consisted of 96 genes upregulated by both SA and cool temperatures, with GO enrichment for 'SAR,' 'response to SA,' and various defense responses (Fig. 4E). The second group (16 genes) was upregulated at below-ambient temperatures, but repressed by SA, and enriched for the GO term 'response to cold.' Indeed, transcript levels of all leaf-expressed COR genes were significantly higher at 18°C than at 22°C in all three genotypes (Fig. 4F). However, the magnitude of COR gene induction was attenuated by SA, being lowest in F24 and highest in NahG (Fig. 4F). When compared with the WT, COR gene expression was significantly downregulated in F24 and upregulated in NahG at 18°C (Fig. 4F). We observed a similar but weaker trend at 22°C with overall lower COR transcript abundance (Fig. 4F). These results corroborated the findings (Fig. 3) of an inhibitory effect of SA on COR gene expression.

255256

258

259

260

261

262

263

264

265

266

257 Constitutive expression of COR genes rescues the growth defects of hiSA plants

COR proteins stabilize membranes during cellular dehydration, a common response to freezing and several other abiotic stresses (Thomashow, 1999; Thalhammer et al., 2014). The suppression of *COR* genes in the hiSA lines might compromise this protective function at below-ambient temperatures. We therefore sought to test the hypothesis that SA-insensitive expression of *COR* genes can rescue the growth defects in the hiSA lines. We first attempted to overexpress *COR15a*, *COR15b* or both (*COR15ab*) under control of the 35S promoter in WT and F24. All *Pro35S:COR15* transgenic plants in both backgrounds exhibited prolonged leaf expansion and delayed senescence (Fig. S4A–D), consistent with a promotive role of COR15a and COR15b in leaf longevity (Yang et al., 2011). While rosette and biomass growth improved at both 22°C and

16°C (Fig. S4E–G), total SA levels and disease resistance became attenuated in homozygous (T4) F24-*COR15* lines (Fig. S4H–I).

We attributed this flaw to 35S promoter-mediated cosuppression because both the original *Fd-Irp9* and the *COR15* constructs were built on pCambia vectors with double 35S promoters driving the selectable marker and the target genes (see Materials and Methods). Shallow RNA-seq confirmed a potent silencing of the (abundantly expressed) *Fd-Irp9* to background levels in two F24-*COR15ab* lines, along with depleted transcript levels of *PR1* and other SA marker genes (Fig. S4J). However, the relatively less expressed *COR15a* and *COR15b* were not silenced, indicative of dose-dependent differential cosuppression responses (Jorgensen et al., 1996). The results are consistent with the F24-*COR15ab* homozygotes reverting SA levels to WT-like but exhibiting prolonged leaf expansion characteristic of ectopic *COR* expression.

In a second attempt, we examined crosses between *COR15ab* (WT background) and hiSA lines in early generations to obtain proof-of-concept data before the co-suppression effect intensifies in homozygous progeny (Fig. 5). In multiple crosses involving independent transgenic lines, F₁ plant growth, leaf senescence, seed yield, and SA metabolite levels were intermediate of their parents at 22°C (Fig. 5A–C). We identified F₂ individuals which maintained high levels of SA accrual and disease resistance like their hiSA parent, but with vastly improved growth at 16°C (Fig. 5D–F). This supports the hypothesis that severing *COR* suppression by SA could alleviate the growth penalty in hiSA lines.

Next, we remade the constructs for ectopic expression of individual *COR* genes under control of the *ACTIN2* (*ACT2*) promoter in the WT, F24, F31, F36, and *siz1-2* backgrounds, hereafter referred to as *eCORs* (ectopic *CORs*). We chose *COR15a*, *COR15b*, and *COR6.6/KIN2* for two reasons: they were most responsive to cooling in F24 (Fig. 4F) and their encoded proteins reside in different subcellular compartments with distinct-yet-overlapping stress responses (Kurkela and Borg-Franck, 1992; Wilhelm and Thomashow, 1993). Consistent with the proof-of-concept data above, all three *eCOR* genes rescued hiSA and *siz1-2* plant growth to varying degrees (Fig. 6 and Figs. S5-S6). Due to prior experience of unexpected gene silencing, we prioritized our transgenic characterization on growth and SA phenotypes. We measured SA levels from one randomly selected plant per genotype from T2 plants to verify no apparent loss of SA accrual in

hiSA-*eCOR* lines (Fig. S6). We grew two randomly selected homozygous lines from each background-*eCOR* combination for further characterization at 22°C and 16°C under long-day conditions. All *eCOR* transgenic lines in hiSA backgrounds showed prolonged leaf expansion, improved growth, and significantly higher biomass over their respective parental lines at both temperatures (Fig. 6A–D and Figs. S5-S6). Specifically at 16°C, hiSA plants expressing *eCORs* exhibited reduced growth penalty relative to the WT or WT-*eCOR* plants (Fig. 6B, D). All *eCOR* lines showed delayed senescence as previously reported (Yang et al., 2011), which resulted in significantly higher seed yields than their cognate background at 16°C (Fig. 6E) as observed for representative F₁ hybrids of *Pro35S:COR15ab* and hiSA lines (Fig. 5C).

Across all backgrounds and at both temperatures, *eCOR15a* and *eCOR15b* appeared more effective than *eCOR6.6* in rescuing hisSA plant growth (Fig. 6A–E). *eCOR* expression also significantly improved *siz1-2* growth at both temperatures but in many cases the biomass and seed yields were still significantly lower than those of WT or WT-*eCOR* lines (Fig. 6A-E), suggesting partial rescue. This along with the observation that SA levels were partially depleted in the *siz1-2* background (Fig. S6) again attests to SA accumulation as a pleiotropic phenotype of *siz1-2* (Park et al., 2011; Kim et al., 2021).

Ectopic expression of *COR* genes did not interfere with resistance to *Pst* DC3000 in the F24 and F31 backgrounds (Fig. 6F–G, Fig. S6), consistent with sustained SA levels in hiSA-*eCOR* lines at either temperature (Fig. 6H and Fig. S6). Furthermore, ion leakage was significantly lower in the F24-*eCOR15a* lines than in the F24 parent and equivalent to that of the WT or WT-*eCOR15a* lines at 16°C (Fig. 6I). Together, the data suggest that it is possible to rescue hiSA plant growth by ectopic *COR* expression to restore membrane protection without compromising SA-mediated disease resistance.

Discussion

The transgenic hiSA Arabidopsis lines reported here permitted unambiguous determination of SA effects on plant growth and stress responses. We show that elevated SA levels reduced

biomass accrual, promoted precocious flowering and senescence, decreased seed yield, improved disease resistance, and enhanced abiotic stress tolerance, all in a dose-dependent manner. Notably, the hiSA lines exhibited more pronounced growth decreases at sub-ambient temperatures. Our data support a model in which SA antagonizes *COR* gene expression to finetune growth and defense responses to external cues (Fig. 7). The SA inhibitory effects appear modest in unstressed plants with basal or low levels of *COR* expression (Fig. 4F, Fig. 7A, top). With decreasing temperatures, *COR* genes are strongly stimulated but this induction is attenuated in hiSA plants (Fig. 4F), which exacerbates the growth reduction (Fig. 7A, bottom). A similar mechanism may also underlie plant responses to a range of biotic and abiotic stresses that activate SA and/or *CORs* to varying extents (Fig. 7A, right). We show that the SA inhibition of growth can be fully or partially rescued by transcriptional rewiring of individual *COR* genes to balance growth and defense (Fig. 7B).

COR proteins were originally identified by their rapid and strong induction in cold-acclimated Arabidopsis (Gilmour et al., 1988; Hajela et al., 1990; Kurkela and Franck, 1990). Several of them were independently discovered in other screens with alternative names, such as cold-inducible (KIN), low temperature-induced (LTI), responsive to desiccation (RD), or early responsive to dehydration (ERD) (*i.e.*, COR6.6 = KIN2; COR47 = RD17; COR78 = LTI78 = RD29a) (Thomashow, 1999). Perhaps less recognized is the sensitivity of *COR* genes to moderate cooling. Wang and Hua (2009) reported *COR* gene induction within hours of cooling (28 \rightarrow 22°C or 22 \rightarrow 16°C), though it was smaller, transient, and more variable than after cold shock (22 \rightarrow 4°C). Among our other findings in this report, we show significant and sustained induction across all *COR* gene families in plants grown at sub-ambient temperatures (Fig. 4F). The work adds to the known dehydration-related abiotic stresses that induce *COR* gene expression.

Cold temperatures reduce plant growth while increasing SA production and disease resistance (Scott et al., 2004; Carstens et al., 2014; Ibañez et al., 2017; Wu et al., 2019; Li et al., 2020). Moderate cooling also reduced plant growth but did not have large effects on SA accrual (similar levels at 22°C and 16°C, Fig. S3) as previously reported (Li et al., 2020; Bruessow et al., 2021). Cooling stimulated *PR* gene expression in an SA-dependent manner, but SA is not required for

cooling-induced COR expression (Wang and Hua, 2009; Kim et al., 2013) (Fig. 4F). Instead, we show that SA had a detrimental effect on the induction of COR and other low-temperature sensitive genes (Fig. 4F). This negative regulation of COR genes by SA has received little attention in the literature, but a majority (58) of the 100 SA-repressed genes we identified, including several CORs (Fig. 3A), was classified as down-regulated by SA or SA-analogs in a meta-analysis (Zhang et al., 2020). Furthermore, an inverse relationship between basal SA levels. and COR transcript abundances was gleaned from different Arabidopsis accessions where levels of COR genes were one to two orders of magnitude higher in Col-0 than C24 at midday (Miller et al., 2015). Diurnal expression of luciferase (LUC) under control of the COR78 promoter was demonstrated in both accessions and the expression amplitudes were much higher in Col-0 than C24 for both COR78(Col):LUC and COR78(C24):LUC transgenes (Miller et al., 2015). The authors suggested that genetic backgrounds act in trans to modulate COR78 expression (Miller et al., 2015). We argue that constitutively elevated SA in C24 (Bechtold et al., 2018) could underlie the suppression of COR genes relative to Col-0. Thus, multiple lines of evidence from the present and previous investigations support an inhibitory role of SA on COR expression in Arabidopsis.

SA and *CORs* have opposing roles in leaf senescence and longevity (Yang et al., 2011; Zhang et al., 2013; Zhang et al., 2017). We posit that SA suppression of CORs likely contributed to the accelerated leaf senescence and flowering phenotypes in our hiSA plants (Fig. 1). This may represent an evolutionary strategy to optimize reproductive success in response to pathogen infection (Korves and Bergelson, 2003). While SA has been implicated in both biotic and abiotic defense (Rivas-San Vicente and Plasencia, 2011; Miura and Tada, 2014; Peng et al., 2021), *COR* genes have mainly been associated with dehydration-related abiotic stress responses (Thomashow, 1999; Miller et al., 2015). Our finding of SA-*COR* regulation thus links CORmediated abiotic (including cooling) responses with SA defense signaling, and adds to the growing network of defense pathway interactions in response to diverse external and internal signals (Aerts et al., 2021; Liu et al., 2022).

Furthermore, the functional pleiotropy of CORs is linked to different regulatory circuits. Whereas COR induction by cold, drought, and other dehydration stresses is regulated by CBFs/DREBs and/or ICEs (Liu et al., 1998; Novillo et al., 2007; Kim et al., 2015; Tang et al.,

2020; Li et al., 2024), COR involvement in leaf longevity is regulated by NAC transcription factor VNI2 (VND-INTERACTING 2) (Yang et al., 2011). Interestingly, VNI2 expression was insensitive to SA or cooling in the present study, suggesting the involvement of other transcription factors in SA-COR regulation of leaf senescence and longevity. As discussed above, cold-activated disease resistance is SA-dependent (Wu et al., 2019; Li et al., 2020). It has been shown that cold and pathogen defense signaling pathways share common players such as membrane receptors, calcium channels, reactive oxygen species, and MAPK (mitogen-activated protein kinase) cascades (Browse and Xin, 2001; Ding et al., 2019; Wu et al., 2019). Specifically, ICE1 has recently been shown to physically interact with NPR1 and TGA3 (TGACG-BINDING FACTOR3) to activate SA signaling during cold-enhanced immunity (Li et al., 2024). However, expression of these genes was unaffected by SA or sub-ambient temperatures in the current study, although their involvement at post-transcriptional levels cannot be excluded. Whether the SA-COR regulation involves CBFs/DREBs, ICEs, or other transcription factors warrants further research. Given that leaf senescence is governed by an interplay of hormonal, developmental, and environmental cues (Jibran et al., 2013; Kim et al., 2017), the involvement of other defense-hormone crosstalk in the SA-COR regulation also requires further research.

All *COR* genes are present as tandem duplicates in Arabidopsis and closely related taxa that predate Brassicaceae speciation (Murat et al., 2015). As such, differences in basal expression (Fig. 4F) and stress responsiveness between paralogs have been reported. For instance, drought induces expression of *COR15a* and *COR6.6* (*KIN2*), but not *COR15b* or *KIN1* (Kurkela and Borg-Franck, 1992; Wilhelm and Thomashow, 1993). The *COR78* tandem duplicates (*RD29a* and *RD29b*) also show different basal expression and stress responsiveness (Yamaguchi-Shinozaki and Shinozaki, 1993). At the protein level, COR proteins vary in size and subcellular localization (*e.g.*, chloroplast for COR15 and cytosol for COR6.6), but they share characteristics of certain late embryogenesis abundant (LEA) and dehydrin proteins, being highly hydrophilic and boiling stable (Gilmour et al., 1996; Kovacs et al., 2008; Thalhammer et al., 2014). Experimentally characterized COR15a and COR15b are unstructured in their fully hydrated state and form amphipathic α-helices upon dehydration to promote membrane association and stabilization (Thalhammer and Hincha, 2014; Navarro-Retamal et al., 2016). Similarly, another

SA-suppressed and low temperature-induced gene LTI30 (Fig. 4F) encodes an intrinsically disordered dehydrin with Lys-rich segments that can fold into α -helices on the lamellar bilayer to stabilize membrane structures (Eriksson et al., 2011; Andersson et al., 2020). The other COR proteins are also predicted as intrinsically disordered hydrophilic proteins with amphipathic α -helical regions (Thomashow, 1999), which suggests that they too may contribute to membrane protection.

Given the overlapping but nonidentical properties of *COR* genes and their encoded proteins and given the widespread suppression of *CORs* by SA, it may seem surprising that transcriptional rewiring of individual *COR* genes was sufficient to restore hiSA plant growth. Nevertheless, the results align with the notion that genetic redundancy underlies both evolvability and robustness of biological systems (Stelling et al., 2004; Kafri et al., 2009; Hunter, 2022). The COR family exemplifies functional redundancy that can arise from duplicated genes (*e.g.*, tandem duplicate) or distinct genes (*e.g.*, different CORs) with overlapping function to buffer against stochastic perturbations, thereby increasing robustness and evolvability of the organism (Hartman et al., 2001; Stelling et al., 2004). *CORs* and other *LTIs* thus constitute a repertoire of "redundant genes" that can compensate for each other's loss (Kafri et al., 2009). In this context, our findings that any of the three *COR* genes tested could fully or partially rescue growth of hiSA mutants are not unexpected, after all.

There are precedents for successful uncoupling of growth-defense trade-offs mediated by another defense hormone, jasmonic acid (JA). JA inhibits growth by antagonizing gibberellin (GA) signaling in both dicot and monocot species (Yang et al., 2012; Heinrich et al., 2013). Accordingly, GA3 supplementation rescued growth defects of JA-activated wild tobacco (*Nicotiana attenuata*) caused by herbivory, MeJA treatment, or genetic lesions in the JA signaling pathway without affecting defense (Heinrich et al., 2013; Machado et al., 2017). In Arabidopsis, the growth penalty of a JA-hyperactivated mutant *jazQ* defective in five JAZ (jasmonate ZIM domain) transcription repressors can be neutralized by another mutation in *PHYB* encoding the shade receptor phytochrome B (Campos et al., 2016). phyB suppresses both GA and growth-promoting phytochrome-interacting factors (PIFs), and its mutation in *jazQ* relieves the GA and PIF suppression in a manner similar to the shade avoidance response to

promote growth (Campos et al., 2016). Thus, select de-repression with JA, GA, and light signaling networks via genetic or pharmacological means can alter growth-defense trade-off outcomes in ways that allow plants to maintain heightened insect defense and robust growth (Heinrich et al., 2013; Campos et al., 2016).

These studies elegantly demonstrated that the growth-defense trade-off is not merely constrained by carbohydrate reserves or energetically costly production of defense compounds (Heinrich et al., 2013; Campos et al., 2016; Machado et al., 2017). Instead, they support the alternative view postulated by Kliebenstein (2016) that growth-defense trade-offs are driven by negative interactions among intersecting signal transduction pathways. In a striking analogy, we show that de-repression of *CORs* can overcome the growth-defense trade-off mediated by SA. While the underlying regulatory circuit remains to be illuminated, the negative regulation of *CORs* by SA exemplifies another "hardwired" transcriptional interaction (Campos et al., 2016) which we posit to restrict leaf longevity upon activation of SA defense signaling.

The collection of hiSA transgenic lines reported here greatly aided in the molecular dissection of the trade-off between growth and SA-mediated defense. SA, a plant defense elicitor, has motivated development of structural analogs for commercial applications, but yield penalties have dampened the prospects of SA-based crop protection in agriculture (Walters et al., 2013). The finding that overriding SA inhibition through constitutive *COR15a*, *COR15b*, or *COR6.6* expression was sufficient to restore plant growth while retaining SA-endowed disease resistance suggests that a minimalist strategy can be effective for genetic improvement of crop productivity. The discovery of genes coordinately and oppositely regulated by cold and SA means that additional molecular targets can be exploited, in a combinatorial and iterative fashion, to decouple growth–defense trade-offs in diverse crops under changing climate conditions. We anticipate that the hiSA transgenic lines will be valuable for mechanistic investigation of SA crosstalk with other phytohormone and defense pathways.

Materials and Methods

Plant materials and growth conditions

Arabidopsis thaliana Columbia-0 (Col-0) accession, cpr5-2, dnd1, siz1-2, and srfr1-4 seeds were 485 obtained from the Arabidopsis Biological Resource Center (ABRC, Columbus, OH, USA). 486 Transgenic NahG seeds in the Col-0 background (Reuber et al., 1998) were a gift from Frederick 487 Ausubel, Massachusetts General Hospital. Seeds were stratified for three days at 4°C and sown 488 onto 5 cm square plastic pots containing Miracle-Gro Moisture Control potting soil (Miracle-Gro 489 Lawn Products, Inc., Marysville, OH, USA) supplemented with Steinernema feltiae (Nemasys, 490 491 BASF Corp., Research Triangle Park, NC, USA). Unless otherwise noted, plants were grown in a Conviron chamber (Conviron Ltd., Winnipeg, Canada) at 22°C with 65W T8 cool-white 492 fluorescent bulbs under a 16 h light (100 µmol m⁻² s⁻¹) and 8 h dark photoperiod. Temperature 493 experiments of soil-grown plants were conducted using two growth chambers set at constant 494 26°C, 22°C, or 16°C, or variable 22°C:18°C or 18°C:16°C day:night temperatures as indicated. 495 Plants were grown under ambient (22°C) conditions until 14 DAG before half of them were 496 transferred to the cool temperature growth chamber. Transgenic plant selection in tissue culture 497 was carried out in a walk-in growth room maintained at 22°C outfitted with 60W FLAT PANEL 498 VEG (FPV24-A) LED lighting (Barron Lighting Group, Glendale, AZ, USA) at 16 h light (100-499 120 μmol m⁻² s⁻¹) and 8 h darkness. Cool temperature experiments of tissue-cultured plants were 500 conducted using a Percival growth chamber (CU36L4, Percival Scientific, IA, USA) set at a 501 constant temperature of 16°C under a 16 h light (SciWhite® PetriClearTM 502 100 μmol m⁻² s⁻¹) and 8 h dark photoperiod. 503

504

505

506

507

508

484

Nicotiana benthamiana seeds obtained from the National Tobacco Germplasm Collection were sown on soil as above and maintained in a walk-in growth room at 22°C with 16 h lighting at 400 μ mol m⁻² s⁻¹ provided by AgroLED® iSunlight® T5 White LED lamps. Plants approximately 2-month-old were used for leaf infiltration.

509

510

511

512

513

514

Generation of transgenic Arabidopsis lines

Transgenic lines were produced via floral dip transformation (Clough and Bent, 1998) using *Agrobacterium tumefaciens* strain C58 (Koncz and Schell, 1986) carrying different binary constructs. To generate the *Fd-Irp9*-OE lines (Supplementary Data Set S3), Col-0 was transformed with the binary plasmid pCAMBIA1302-*Pro35S:Fd-Irp9* (Xue et al., 2013). T₁

plants were selected on half-strength Murashige and Skoog (1/2 MS) medium with 20 mg L⁻¹ hygromycin and confirmed by PCR using primers for *Irp9* and *HPT* encoding hygromycin phosphotransferase (Table S1). Confirmed T₁ plants were transplanted to soil for LC-MS screening of SA levels (see below) and seeds from selected lines were harvested. T₂ plants were again confirmed by PCR as above and by LC-MS analysis of SA metabolites, and T₃ seeds were harvested for antibiotic screening of homozygous lines. T₃ and T₄ plants were again analyzed for SA levels by LC-MS. From the first pilot transformation trial, one hiSA event was recovered (F24). Then, a larger T₁ population from a second transformation trial was screened to select a panel of lines that represent a wide range of SA increases for further characterization.

For preparation of Pro35S: COR15 constructs, the coding sequences of COR15a (At2g42540, ABRC stock no. U12858) and COR15b (At2g42530, stock no. U10423) were PCR-amplified using primers containing vector homology (Table S1). The cDNAs were cloned into SpeI and PmlI digested pCM (modified from pCAMBIA2301, Swamy et al., 2015) via Gibson assembly (NEBuilder HiFi DNA Assembly Cloning Kit, NEB, Ipswich, MA, USA) and sequence verified to generate Pro35S: COR15a and Pro35S: COR15b constructs. For the construct containing both COR15a and COR15b (COR15ab for short), the COR15a cassette was PCR-amplified using primers with vector homology (Table S1) and cloned into Pro35S:COR15b predigested with EcoRI and BamHI to produce Pro35S: COR15a-Pro35S: COR15b (Pro35S: COR15ab) which was sequence confirmed. Floral dip transformation of WT and F24 was performed as above and transgenic plants were selected by 50 mg L⁻¹ kanamycin without (WT background) or with 20 mg L⁻¹ hygromycin (F24 background). T₁ plants obtained from antibiotic selection were confirmed by PCR using NPTII (neomycin phosphotransferase II) and transgenic COR-vector primers (Table S1). T₃ plants were again PCR-checked using Irp9, HPT, NPTII, and transgenic COR-vector primers and tested for disease resistance (see below). Homozygous T₄ plants were grown at 22°C and 16°C for biomass, SA measurements, and disease resistance analysis (only the 22°C group).

A second set of *COR15a* and *COR15b* vectors was similarly prepared using primers that introduced sequences encoding C-terminal HA-tag and Strep-tag II, respectively (Table S1). A *COR6.6* (At5g15970)-*Flag* fragment was synthesized as gBlocks (Integrated DNA

Technologies, IA, USA) and cloned into pCM as described above. To avoid transgene co-suppression, the Pro35S:COR15a-HA, Pro35S:COR15b-StrepII, and Pro35S:COR6.6-Flag cassettes were PCR-amplified and Gibson-assembled into a SpeI/PmeI-digested p201N backbone (Addgene #59175) in which the kanamycin selection marker gene was controlled by the potato (Solanum tuberosum) Ubiquitin3 promoter and terminator (Jacobs et al., 2015). The 35S promoter was swapped for the Arabidopsis ACTIN2 (ACT2) promoter amplified from clone pAtA2pt-Ppo (a gift from Peter Lafayette, University of Georgia, Athens, GA, USA) by Gibson assembly to generate *ProACT2:COR* constructs. All constructs were verified by sequencing.

Arabidopsis floral dip transformation was performed as above in WT, F24, F31, F36, and *siz1-2* backgrounds and transgenic plants were selected by 50 mg L⁻¹ kanamycin with 20 mg L⁻¹ hygromycin (in hiSA backgrounds) or without (WT and *siz1-2* backgrounds). T₁ plants were further screened by PCR using *Irp9*, *HPT*, *NPTII*, and transgenic *COR*-vector primers (Table S1). T₂ plants were selected based on antibiotic resistance and increased leaf longevity characteristic of ectopic *COR* expression. Two randomly selected events per construct in each background were analyzed by LC-MS for SA levels and advanced through T₃ to obtain homozygous plants. Homozygous plants were grown at 22°C and 16°C for growth characterization, and a subset of plants were used for SA measurements and disease resistance analysis (see below).

Growth monitoring and biomass analysis

Col-0 WT, homozygous Fd-Irp9-OE lines, NahG, and several autoimmune mutants were monitored for various growth parameters shown in Fig. 1. Rosette leaf (nos. 7-8) thickness and rosette canopy diameter of plants grown at 22°C (n = 5 plants) were measured at bolting stage 5.1 (28 DAG) according to Boyes et al. (2001) and the plants were destructively harvested for rosette and root biomass. The number of lateral roots (> 1 cm) was counted and dry weight was obtained after oven drying at 55°C. Additional plants (n = 5) were monitored for the onset of leaf senescence and bolting. Seed yield and silique traits (number and length) were measured at 50 DAG. Similar growth monitoring experiments were conducted more than 10 times, including as background genotypes for subsequent Pro35S:COR and ProACT2:COR transformants, with reproducible trends.

Growth comparison at 22°C and 16°C of WT, NahG, and Fd-Irp9-OE lines was similarly performed using n = 8 plants for data shown in Fig. 4C, or n = 4 plants for replicate data shown in Fig. S3B. Similar growth monitoring experiments were performed at least four times, including as background genotypes for subsequent Pro35S:COR and ProACT2:COR experiments, with reproducible patterns. The comparison among WT, NahG, and F24 was conducted more than 10 times under various growth temperatures from 16°C to 26°C. Growth monitoring of Pro35S:COR or ProACT2:COR transformants (two randomly selected events per group) was conducted using n = 3-4 homozygous plants, except when F1 and F2 progeny from selected crosses were used. The experiments were performed once for Pro35S:COR plants and at least three times for ProACT2:COR transformants with similar trends. Biomass data were measured only once as shown in Fig. 6 from 30 DAG plants at 22°C and 40 DAG at 16°C. Statistical significance between each transgenic group and WT or between each transgenic COR line and its cognate background was determined using two-sided Student's t-test.

592 RNA-seq analysis

Three fully expanded rosette leaves (no. 7–9) per plant were snap-frozen in liquid nitrogen. Plants at growth stage 5.1 (Boyes et al., 2001) were used, which corresponded to 30 DAG at 22°C (Fig. 3, Dataset S1) and 28 DAG at 22° C or 38 DAG at 18° C (Fig. 4E–F, Dataset S2) in two separate experiments. Approximately 50-100 μ L volume of liquid nitrogen-ground powder was used for RNA isolation with a Direct-zol RNA MiniPrep Kit (Zymo Research, Irvine, CA, USA) and PureLink Plant RNA Reagent (Invitrogen, Waltham, MA, USA). RNA library preparation and Illumina NextSeq 500 sequencing (single end, 75 cycles) were performed at the Georgia Genomics and Bioinformatics Core of the University of Georgia (Supplementary Data Set S3). Sequence data were preprocessed as described previously (Xue et al., 2015) and mapped to the *Arabidopsis thaliana* TAIR v10 reference genome using STAR v2.5.3a (Dobin and Gingeras, 2015). Transcript abundance was estimated by featureCounts v1.5.2 (Liao et al., 2014) for differential expression analysis by DESeq2 v1.22 with multiple testing corrections (Love et al., 2014). Differentially expressed genes were determined by RPKM \geq 3, $Q \leq$ 0.05, and fold-change \geq 1.5 using n = 4 plants (individual pools of three rosette leaves per plant per pool), except one contaminated F51 sample (Fig. 3 and Dataset S1) that was mis-clustered with *NahG*

samples in principal component analysis and was excluded. Only nuclear protein-coding genes were reported. Log₂-adjusted expression values were z-score transformed for hierarchical clustering analysis using Morpheus (https://software.broadinstitute.org/morpheus) with Pearson's correlation as the distance metric. Gene ontology enrichment was performed using ShinyGO v0.76.3 (Ge et al., 2020). Venn diagrams were drawn with DeepVenn (Hulsen, 2022), and expression ratios were visualized with HeatMapper Plus (https://bar.utoronto.ca/ntools/cgibin/ntools heatmapper plus.cgi).

614615

616

617

618

619

620

621

622

623

624

625

626

627

628

629

630

631

632

633

634

635

636

637

608

609

610

611

612

613

Metabolite analysis

SA metabolites were measured by reverse-phase high-performance liquid chromatography—mass spectrometry (HPLC–MS) as detailed previously (Xue et al., 2013) using plants at bolting (stage 5.1). For screening of early generation transformants, one fully expanded rosette leaf (no. 8) was sampled using a biopsy punch (2 mm diameter) directly into the extraction buffer. For analysis of homozygous transgenic lines, rosette leaves (nos. 7-9) were flash-frozen in liquid nitrogen, ground to a fine powder, and an aliquot freeze-dried. Four leaf discs or 5 mg of freeze-dried leaf powder per plant was extracted in 200 µL of extraction buffer (1:1 methanol:chloroform, v v⁻¹) containing ¹³C₆-cinnamic acid, D₅-benzoic acid, and resorcinol as internal standards. Metabolite identity was confirmed with authentic standards for SA, 2,3-DHBA, 2,5-DHBA (Sigma-Aldrich, St. Louis, MO, USA) and SAG (Toronto Research Chemicals, Toronto, ON, Canada), previously fraction-collected compounds for 2,5-DHBG and SGE (Xue et al., 2013), or through MS fragmentation match against published data or NIST library for 2,5-DHBX, 2,3-DHBG, and 2,3-DHBX (Dean and Delaney, 2008; Bartsch et al., 2010; Xue et al., 2013). The glycosides and xylosides were further confirmed by LC-MS and tandem MS analysis of Nicotiana benthamiana extracts from leaves infiltrated with 1 mM SA, 2,3-DHBA, or 2,5-DHBA (Fig. S2). Except for the T_1 screening (n = 1) and when noted otherwise, SA metabolite analysis of Fd-Irp9-OE lines was performed with n = 7-12 (T₂) or n = 5-8 (homozygous) plants. The experiment with homozygous hiSA lines at ambient temperatures was performed at least four times with reproducible trends. Experiments comparing 22°C and 16°C plants were conducted twice with similar patterns. SA metabolite analysis of Pro35S:COR or ProACT2:COR transformants was performed with n = 6 (Pro35S:COR) or n = 5 (ProACT2:COR) individual plants, except for the

- confirmation analysis of *ProACT2:COR* T_2 lines (n = 1 plant per line) in all genetic backgrounds.
- Statistical differences were determined by two-sided Student's t-test against WT samples.

- 641 Pathogenicity assay
- Plant resistance to *Pseudomonas syringae* pv. tomato strain DC3000 (*Pst* DC3000) was assessed
- for soil-grown plants under the specified conditions using syringe infiltration of rosette leaves as
- described previously (Lovelace et al., 2018). Two days before inoculation, *Pst* DC3000 cultures
- were grown in King's B medium (Sigma-Aldrich, St. Louis, MO, USA) supplemented with 50
- mg L⁻¹ rifampicin. Pst DC3000 inoculum was prepared at a concentration of 1×10^6 colony-
- forming units (CFU) mL^{-1} (OD₆₀₀ = 0.1, diluted 1:100) in 25 mM magnesium chloride. Rosette
- leaves 7 and 8 were inoculated with bacterial suspensions. Two days post-inoculation (DPI), four
- leaf discs (two discs per leaf) were collected from each infiltrated plant and homogenized for 2
- min in 500 µL of 25 mM magnesium chloride in a SpeedMill PLUS Bead Mill homogenizer
- 651 (Analytik Jena AG, Jena, Germany). Homogenized samples were serially diluted, and 10 μL of
- each dilution was plated on King's B medium containing 50 mg L⁻¹ rifampicin. CFU were
- counted after two days of incubation at 28°C, and data are presented as log₁₀ CFU cm⁻² (Fig.
- 654 2A). The experiment was performed six times for Fd-Irp9-OE lines (n = 3 plants) at 22°C with
- similar results, including as background genotypes for the Pro35S:COR or ProACT2:COR
- 656 transformants. The experiment for the *Pro35S:COR* transformants (*COR15a*, *COR15b*, and
- 657 COR15ab) was conducted once in T_3 and once in T_4 (n = 3 plants), showing gradual loss of
- disease resistance in the F24 background due to co-suppression (Fig. S4I). The experiment for
- 659 ProACT2:COR transformants (COR15a, COR15b, and COR6.6) in various backgrounds (n = 4
- plants) was conducted once at 22°C (Fig. 6F). Statistical significance was determined by two-
- sided Student's t-test against WT or their respective background genotype as indicated.

- Resistance to Pst DC3000 was also evaluated by flood-inoculation assays as described
- previously (Ishiga et al., 2011) using *in-vitro-*cultured plants. After surface sterilization and
- stratification for 48 h at 4°C, seeds sown on half-strength MS medium with 0.3% (w v⁻¹) gellan
- gum (PhytoTechnology Laboratories, Shawnee Mission, KS, USA) were incubated at 22°C with
- a 16 h light (100-120 μmol m⁻² s⁻¹) and 8 h darkness photoperiod. Four days after germination,
- seedlings were transferred to pathogenicity-assay Petri dishes each containing five seedlings

from different genotypes. Two days before inoculation, Pst DC3000 culture was prepared as above in 25 mM magnesium chloride containing 0.025% (v v⁻¹) Silwet L-77. Two-week-old Arabidopsis seedlings were flooded with 20 mL of inoculum for 3 min. After removal of excess bacteria, plates were sealed with Micropore surgical tape (3M, St. Paul, MN, USA) and incubated under normal growth conditions. At 3 DPI, rosettes were surface-sterilized by plate flooding with 20 mL of 5% (v v⁻¹) hydrogen peroxide for 3 min, followed by washing three times with sterile dH₂O. After blotting dry on sterile paper towels, three leaves per plant were weighed and homogenized as above and serial dilutions plated. CFU were counted after two days of incubation at 28°C, and data are presented as \log_{10} CFU mg⁻¹ fresh weight tissue. The experiment was performed in a randomized complete block design where each Petri plate of 5–7 genotypes (one plant per genotype) was an experimental unit and five biological replicates per genotype were included (n = 5 plants). The experiment for Fd-Irp9-OE lines was conducted twice with similar patterns (Fig. 2B). Statistical significance was determined by two-sided Student's t-test against WT samples. The seedling flood-inoculation assays were conducted once for the F₂ progeny of Pro35S: COR15ab2 × F31 at 22°C (Fig. 5F) and once for the F24-eCOR lines at 16°C (Fig. 6G and Fig. S6C). For the latter, tissue cultured plants (seven genotypes per plate, three plants per genotype) were prepared as above and grown at 22°C for 10 days before transferring to a 16°C growth chamber. Bacterial inoculation was performed 11 days after (3week-old plants) for visual documentation of disease responses (Fig. 6G and Fig. S6C).

687 688

689

690

691

692

693

694

695

696

697

698 699

669

670

671

672

673

674

675

676

677

678

679

680

681

682

683

684

685

686

Abiotic stress assays

Surface-sterilized *NahG*, Col-0, F19, F24, F36, and *siz1-2* seeds were germinated as described and four-day-old seedlings were transferred to vertically placed square Petri dishes (Simport, Quebec, Canada) containing half-strength MS alone or with 100 mM NaCl or 250 mM mannitol. Primary root length was measured on eleven-day-old seedlings. The experiment consisted of five replicate plates per treatment group, each plate containing two seedlings per genotype. The experiment was performed twice with similar results. For plant response to methyl viologen (or paraquat dichloride; Sigma, St. Louis, MO, USA), surface-sterilized and stratified seeds were plated on half-strength MS either alone or containing 5 μM methyl viologen. The plates were incubated at 22°C with 16 h light (100-120 μmol m⁻² s⁻¹). Germination response was recorded seven days after sowing. The experiment consisted of five replicate plates per group, each with

10 seeds per genotype. The experiment was performed twice with similar results. Statistical significance was determined by two-sided Student's *t*-test against WT samples.

701702

703

700

Ion leakage assays

Four 2 mm leaf discs (rosette leaf 8) per plant (n = 5 plants) were collected into 15 mL Falcon tubes containing 5 mL of ddH₂O. Samples were shaken at 60 rpm for 4-6 h at ambient temperature. Conductivity was measured using a conductivity meter (Traceable Products, Friendswood, TX, USA). The samples were boiled for 30 min and cooled to room temperature, and conductivity was measured again as total ion leakage. Conductivity values were corrected using ddH₂O as a blank. Ion leakage for each genotype was estimated from initial conductivity as a percentage of total conductivity. The genotype, temperature, and genotype × temperature effects were determined by two-way ANOVA, and significant effects were analyzed post-hoc with Tukey's honestly significant difference (HSD) test using JMP Pro 16 (SAS Institute, Cary, NC, USA). The experiment was conducted once. The effects of ectopic *COR15a* expression in WT or F24 background on ion leakage were similarly assessed for tissue-cultured plants grown at 16°C, using six 2 mm leaf discs from rosette leaf 8 per plant (n = 5 plants). Statistical significance was determined by two-sided Student's *t*-test against WT and, for F24-*eCOR* lines, against the F24 background as well. This experiment was performed once.

Statistical Analysis

Statistical analyses were performed as described in each figure legend. Statistical data are provided in Supplementary Data Set S3.

704

705

706

707

708

709

Accession numbers

Accession numbers of the genes used in this study are: *ACT2* (AT3G18780), *COR6.6* (AT5G15970), *COR15a* (AT2G42540), *COR15b* (AT2G42530), *FD* (At1g60950), and *Irp9* (CAB46570). RNA-seq data are available from the NCBI SRA under accession numbers PRJNA939115 and PRJNA942941.

710711

Supplementary Data

- Supplementary Figure S1. SA metabolite analysis of T₁, T₂, and T₃ Fd-Irp9-OE plants (Supports
- 713 Figure 1).
- Supplementary Figure S2. LC-MS chromatograms and MSMS fragmentation patterns of SA-
- 715 derived metabolites (Supports Figure 1).
- Supplementary Figure S3. SA metabolite levels and growth of *Fd-Irp9*-OE plants at 22°C or
- 717 16°C (Supports Figure 4).
- Supplementary Figure S4. Characterization of homozygous F24-*Pro35S:COR* transformants
- 719 (Supports Figure 5).
- Supplementary Figure S5. Growth phenotypes of additional *ProACT2:COR* transgenic lines
- 721 (Supports Figure 6).
- Supplementary Figure S6. Additional phenotypes of *ProACT2:COR* transformants (Supports
- 723 Figure 6).
- Supplementary Table S1. Primers used in this study.
- Supplementary Data Set S1. Differentially expressed genes in response to SA changes at 22°C.
- Supplementary Data Set S2. Differentially expressed genes in response to SA and below-ambient
- 727 temperatures.

734

739

Supplementary Data Set S3. Results of statistical analyses.

730 **Funding information**

- This work was partially supported by the Georgia Research Alliance-Hank Haynes Endowment,
- the National Science Foundation (DBI-0836433 and IOS-2039313), and the National Institute of
- 733 Food and Agriculture (2021-70410-35297).

735 Acknowledgments

- We thank Kate Tay, Jacob Reeves, Thomas Horn, Slisha Shrestha, Dionne Martin, Batbayar
- Nyamdari, Khadijeh Mozaffari, Brent Lieb, and Ran Zhou for laboratory and analytical
- assistance and Scott Harding and Li Yang for insightful discussion.
- 740 Competing interests: The University of Georgia Research Foundation has submitted a patent
- application on behalf of C.J.T. and M.A.O. All other authors declare that they have no competing
- 742 interests.

Author contributions

- Y.Y., C.J.T., and M.A.O. conceived and designed the experiments; M.A.O. and R.M.C.
- performed research experiments with assistance from F.C., M.R.D., and S.P.P.; Y.Y. and B.H.K.
- contributed reagents; M.A.O., R.M.C., L.J.X., B.H.K., and C.J.T. analyzed and discussed the
- data; M.A.O. drafted the paper and C.J.T. revised the paper.

749

743

744

750

751

Figure legends

Fig. 1. Characterization of the Arabidopsis Fd-Irp9-OE lines. (A) Simplified diagram of Irp9mediated SA biosynthesis and downstream catabolism and conjugation. (B) Representative plant morphology 45 days after germination (DAG) at 22°C. Inset shows juvenile senescence of cpr5-2 not seen in F24. Scale bars, 1 cm. (C) Levels of SA-derived conjugates in rosette leaves of wild type (WT), homozygous Fd-Irp9-OE lines, and autoimmune mutants at bolting. Data are means \pm SD of n = 5 independent pools, each sampled from three rosette leaves per plant. (D–F) Vegetative growth traits at 28 DAG (D), onset of senescence (E) and bolting (F) and seed traits at 50 DAG (F). Data are means \pm SD of n = 5 plants. (G) Premature senescence in F24 (right) compared with WT (middle) and NahG (left). Scale bars, 5 cm. (H) Representative images of F24 at seed set (scale bar, 1 cm). Inset shows incompletely developed siliques (scale bar, 0.5 cm). (I) Representative images of seeds. Scale bars, 0.5 mm. Data are means \pm SD of n = 5plants. Statistical significance was determined by two-sided Student's t-test against WT (***P < 0.001; **P < 0.01; *P < 0.05). The growth phenotypes were reproducible in more than 10 experiments. The experiment for SA analysis was conducted four times with similar trends. DHBG, dihydroxybenzoate glucoside; DHBX, dihydroxybenzoate xyloside; SA, salicylic acid; S3H, SA 3-hydroxylase; S5H, SA 5-hydroxylase; SAG, SA glucoside; SGE, SA glucose ester.

Fig. 2. Responses of Fd-Irp9-OE lines to pathogen or abiotic stresses. (A) Pst DC3000 bacterial growth based on leaf infiltration of soil-grown plants at bolting. Data are means \pm SD of n = 3 independent pools of four leaf discs sampled from two rosette leaves per plant. The experiment was performed six times with similar trends. (B) Pst DC3000 bacterial growth based on flood-inoculation of 2-week-old seedlings in tissue culture. Representative plant images from WT and

F31 three days after inoculation are shown. Scale bar, 1 cm. Data are means \pm SD of n=5 independent pools of three rosette leaves per plant. The experiment was performed twice with similar patterns. (C) Primary root growth of 11-day-old seedlings on half-strength MS medium (1/2 MS) alone or with NaCl or mannitol. Data are means \pm SD of n=5 independent pools of two seedlings per pool (each data point was averaged from two seedlings). (D) Seed germination in the presence of methyl viologen. Data are means \pm SD of n=5 independent pools of 10 seeds per pool. The abiotic stress experiments were performed twice with similar results. Statistical significance was determined by two-sided Student's t-test against WT (***P < 0.001; **P < 0.01; *P < 0.05).

Fig. 3. Leaf transcriptomic responses of the Fd-Irp9-OE lines. (A) Hierarchical clustering of 471 SA-responsive genes selected according to differential expression in both F51 and NahG lines relative to the WT. Representative genes that were positively or negatively regulated by SA are shown on the right (*S3H not captured in the list was included for reference). Data were obtained from n = 4 independent pools, each sampled from three rosette leaves per plant at 30 DAG, except for F51 where n = 3 independent pools. Differential expression relative to WT was determined by DEseq2 based on $Q \le 0.05$ and fold-change ≥ 1.5 . Color scale bar denotes the z-score transformed \log_2 ratios. Color scale bar denotes the normalized \log_2 ratio (B) Gene ontology (GO) enrichment of genes positively or negatively regulated by SA. Only GO terms with $-\log_{10}$ FDR > 5 and fold-enrichment > 9 are shown. The RNA-seq experiment was conducted once.

Fig. 4. Temperature-sensitive growth and transcriptomic responses of the Fd-Irp9-OE lines. (A) Representative phenotypes of NahG, WT, and F24 plants at 26°C (18 DAG), $\underline{22}$ °C:18°C (\underline{day} :night, 18 DAG), $\underline{18}$ °C:16°C (\underline{day} :night, 26 DAG), or 16°C ($\underline{22}$ DAG). Scale bars, 1 cm. Each condition was repeated at least once with similar results. (B) Representative phenotypes of NahG, WT, Fd-Irp9-OE (low to high SA, left to right), and siz1-2 plants at 22°C (30 DAG) or 16°C (49 DAG). Scale bars, 1 cm. (C) Regression analysis between total plant biomass and total rosette SA levels of multiple genotypes grown at 22°C or 16°C (n = 8 plants except for F51 at 16°C where n = 7 plants). SA metabolite data are shown in Supplementary Figure S3A. (D) Percent ion leakage of rosette leaf 8 from plants grown at 22°C or 16°C. Data are means \pm SD (n

= 5 plants). Effects of genotype (G), temperature (T), and their interaction were determined by two-way ANOVA, followed by Tukey's post-hoc tests; significance is indicated by letters. The experiments were conducted four times for growth monitoring, twice for SA measurements, and once for ion leakage analysis. (E) Venn diagram of differentially expressed genes in response to SA (NahG vs. WT or F24 vs. WT) at 18° C or to temperature changes (18° C vs. 22° C) in the WT. Clustering analysis of the intersection of 118 genes is shown below, and the top GO terms are indicated on the right. Color scale bar denotes the z-score transformed \log_2 ratios. (F) Expression response heatmaps of COR genes. Values are \log_2 -transformed ratios (significant difference denoted by boldface). Average transcript abundance (reads per kilobase of transcript per million mapped reads, RPKM) of WT samples at 22° C or 18° C is also shown. Data were obtained from n = 4 independent pools, each sampled from three rosette leaves per plant at bolting. Differential expression between the specified sample pair was determined by DEseq2 based on $Q \le 0.05$ and fold-change ≥ 1.5 . The RNA-seq experiment was performed once. NG, NahG.

Fig. 5. F_1 and F_2 progeny phenotypes of Pro35S:COR15ab and hiSA crosses before the onset of silencing. (A–C) Plant growth at 65 DAG (A), total SA metabolite levels measured in leaf punches (B), and seed yield (C) of representative F_1 plants from $COR15ab3 \times F36$ at 22°C. Data for homozygous genotypes are means \pm SD of n = 5 (B) or n = 3 (C) plants. (D–F) Plant growth at 65 DAG at 16°C (D), total SA levels in leaf punches at 22°C or 16°C (E), and Pst DC3000 disease resistance at 22°C of representative F_2 progeny from $COR15ab2 \times F31$ F_1 #7 or #8. Data for homozygous genotypes are means \pm SD of n = 5 (E) or n = 3 (F) plants. Each experiment was performed once. Scale bars, 1 cm.

Fig. 6. Constitutive ProACT2:COR expression rescues growth of SA-hyperaccumulating lines. (A) Mature leaves of representative transgenic plants expressing eCOR15a, eCOR15b, or eCOR6.6 in WT, siz1-2, and hiSA backgrounds at 22°C (30 DAG). Scale bar, 1 cm. Whole plant images are shown in Supplementary Figure S6A. (B) Plant growth of representative eCOR transgenic lines (49 DAG) at 16°C. Scale bar, 1 cm. (C–E) Rosette biomass (C–D) and seed yield (E) at 22°C (C) or 16°C (D–E) from two events per transformation (abbreviated without "eCOR"). Data are means \pm SD of n=4 plants. Statistical significance against the respective background was determined by two-sided Student's t-test (***P < 0.001; **P < 0.01). (F)

Disease resistance against Pst DC3000 based on leaf infiltration of soil-grown plants at 22°C (30 DAG). Data are means \pm SD of n=3 independent pools, each sampled from two rosette leaves per plant per pool. No statistical significance (ns) was found against the respective background based on two-sided Student's t-test. Statistical differences against WT are indicated by asterisks inside the bar (***P < 0.001; **P < 0.01; *P < 0.05). (G) Responses to Pst DC3000 based on flood inoculation of tissue-cultured plants at 16°C. Scale bar, 1 cm. Additional replicates are shown in Supplementary Figure S6. (H–I) Total SA (H) and percent ion leakage (I) in rosettes of tissue-cultured plants at 16°C. Data are means \pm SD (n=5 plants). Statistical significance was determined by two-sided Student's t-test against WT in (H) or as indicated (I) (**P < 0.01; *P < 0.05). The growth experiments were conducted three times with reproducible phenotypes. All other analyses were performed once.

Fig. 7. A proposed model for the growth–defense trade-off involving SA and CORs in response to various stressors. (A) Plant growth under ambient conditions with basal or low levels of *COR* expression (blue arrows) is negatively affected by SA (top). CORs are strongly stimulated for membrane protection at below-ambient temperatures. This induction is attenuated by SA (grey flatheads), resulting in exacerbated growth reduction in hiSA plants (bottom). The negative regulation of *CORs* by SA may also affect growth–defense trade-offs in response to various biotic and abiotic stressors denoted by brown and blue arrows, respectively, on the right. (B) Ectopic expression of individual *COR* genes can bypass SA suppression and rescue plant growth. Scale bars, 1 cm. The COR6.6 and COR15a structural predictions were retrieved from AlphaFold DB (https://alphafold.ebi.ac.uk).

References

Abreu, M.E., and Munné-Bosch, S. (2009). Salicylic acid deficiency in NahG transgenic lines and sid2 mutants increases seed yield in the annual plant Arabidopsis thaliana. Journal of Experimental Botany **60**, 1261-1271.

Aerts, N., Pereira Mendes, M., and Van Wees, S.C.M. (2021). Multiple levels of crosstalk in hormone networks regulating plant defense. Plant J 105, 489-504.

Albrecht, T., and Argueso, C.T. (2017). Should I fight or should I grow now? The role of cytokinins in plant growth and immunity and in the growth–defence trade-off. Annals of Botany **119,** 725-735.

Alcázar, R., and Parker, J.E. (2011). The impact of temperature on balancing immune responsiveness and growth in Arabidopsis. Trends in Plant Science **16**, 666-675.

- Andersson, J.M., Pham, Q.D., Mateos, H., Eriksson, S., Harryson, P., and Sparr, E. (2020).
 The plant dehydrin Lti30 stabilizes lipid lamellar structures in varying hydration conditions [S]. J Lipid Res **61**, 1014-1024.
 - Bartsch, M., Bednarek, P., Vivancos, P.D., Schneider, B., von Roepenack-Lahaye, E., Foyer, C.H., Kombrink, E., Scheel, D., and Parker, J.E. (2010). Accumulation of isochorismate-derived 2,3-dihydroxybenzoic 3-O-beta-D-xyloside in *Arabidopsis* resistance to pathogens and ageing of leaves. Journal of Biological Chemistry **285**, 25654-25665.
 - **Bechtold, U., Ferguson, J.N., and Mullineaux, P.M.** (2018). To defend or to grow: lessons from Arabidopsis C24. Journal of Experimental Botany **69**, 2809-2821.
 - Bhattacharjee, S., Halane, M.K., Kim, S.H., and Gassmann, W. (2011). Pathogen effectors target Arabidopsis EDS1 and alter its interactions with immune regulators. Science 334, 1405-1408.
 - **Bowling, S.A., Clarke, J.D., Liu, Y., Klessig, D.F., and Dong, X.** (1997). The cpr5 mutant of Arabidopsis expresses both NPR1-dependent and NPR1-independent resistance. Plant Cell 9.
 - Boyes, D.C., Zayed, A.M., Ascenzi, R., McCaskill, A.J., Hoffman, N.E., Davis, K.R., and Görlach, J. (2001). Growth stage-based phenotypic analysis of Arabidopsis: A model for high throughput functional genomics in plants. Plant Cell 13, 1499-1510.
 - **Browse, J., and Xin, Z.** (2001). Temperature sensing and cold acclimation. Current Opinion in Plant Biology **4,** 241-246.
 - Bruessow, F., Bautor, J., Hoffmann, G., Yildiz, I., Zeier, J., and Parker, J.E. (2021). Natural variation in temperature-modulated immunity uncovers transcription factor bHLH059 as a thermoresponsive regulator in Arabidopsis thaliana. PLOS Genetics 17, e1009290.
 - Bruggeman, Q., Raynaud, C., Benhamed, M., and Delarue, M. (2015). To die or not to die? Lessons from lesion mimic mutants. Front Plant Sci 6, 24.
 - Campos, M.L., Yoshida, Y., Major, I.T., de Oliveira Ferreira, D., Weraduwage, S.M., Froehlich, J.E., Johnson, B.F., Kramer, D.M., Jander, G., Sharkey, T.D., and Howe, G.A. (2016). Rewiring of jasmonate and phytochrome B signalling uncouples plant growth-defense tradeoffs. Nat Commun 7, 12570.
 - Carstens, M., McCrindle, T.K., Adams, N., Diener, A., Guzha, D.T., Murray, S.L., Parker, J.E., Denby, K.J., and Ingle, R.A. (2014). Increased resistance to biotrophic pathogens in the Arabidopsis constitutive induced resistance 1 mutant is EDS1 and PAD4-dependent and modulated by environmental temperature. PLoS One 9, e109853.
 - Chan, C.W., Schorrak, L.M., Smith, R.K., Jr., Bent, A.F., and Sussman, M.R. (2003). A cyclic nucleotide-gated ion channel, CNGC2, is crucial for plant development and adaptation to calcium stress. Plant Physiol 132, 728-731.
 - **Clough, S.J., and Bent, A.F.** (1998). Floral dip: a simplified method for *Agrobacterium* mediated transformation of *Arabidopsis thaliana*. The Plant Journal **16,** 735-743.
- Clough, S.J., Fengler, K.A., Yu, I.c., Lippok, B., Smith, R.K., and Bent, A.F. (2000). The
 Arabidopsis dnd1 "defense, no death" gene encodes a mutated cyclic nucleotide-gated ion channel. Proc Natl Acad Sci U S A 97, 9323-9328.

- Dean, J.V., and Delaney, S.P. (2008). Metabolism of salicylic acid in wild-type, ugt74f1 and ugt74f2 glucosyltransferase mutants of Arabidopsis thaliana. Physiologia Plantarum 132, 417-425.
- Ding, Y., Shi, Y., and Yang, S. (2019). Advances and challenges in uncovering cold tolerance regulatory mechanisms in plants. New Phytologist 222, 1690-1704.
- Ding, Y., Sun, T., Ao, K., Peng, Y., Zhang, Y., Li, X., and Zhang, Y. (2018). Opposite roles of salicylic acid receptors NPR1 and NPR3/NPR4 in transcriptional regulation of plant immunity. Cell 173, 1454-1467.e1415.
- **Dobin, A., and Gingeras, T.R.** (2015). Mapping RNA-seq reads with STAR. Curr Protoc Bioinformatics **51,** 11.14.11-11.14.19.
- Eriksson, S.K., Kutzer, M., Procek, J., Gröbner, G., and Harryson, P. (2011). Tunable membrane binding of the intrinsically disordered dehydrin Lti30, a cold-induced plant stress protein. Plant Cell 23, 2391-2404.
- Freh, M., Gao, J., Petersen, M., and Panstruga, R. (2022). Plant autoimmunity—fresh insights into an old phenomenon. Plant Physiology **188**, 1419-1434.

827

828

832

833

834

- Ge, S.X., Jung, D., and Yao, R. (2020). ShinyGO: a graphical gene-set enrichment tool for animals and plants. Bioinformatics **36**, 2628-2629.
- Gilmour, S.J., Hajela, R.K., and Thomashow, M.F. (1988). Cold acclimation in *Arabidopsis thaliana*. Plant Physiol **87**, 745-750.
 - **Gilmour, S.J., Lin, C., and Thomashow, M.F.** (1996). Purification and properties of Arabidopsis thaliana COR (cold-regulated) gene polypeptides COR15am and COR6.6 expressed in Escherichia coli. Plant Physiology **111**, 293-299.
- Gu, Y., Zebell, S.G., Liang, Z., Wang, S., Kang, B.-H., and Dong, X. (2016). Nuclear pore permeabilization is a convergent signaling event in effector-triggered immunity. Cell 166, 1526-1538.e1511.
 - **Hajela, R.K., Horvath, D.P., Gilmour, S.J., and Thomashow, M.F.** (1990). Molecular cloning and expression of COR (Cold-Regulated) genes in Arabidopsis thaliana. Plant Physiology **93,** 1246-1252.
- Hartman, J.L., Garvik, B., and Hartwell, L. (2001). Principles for the buffering of genetic variation. Science **291**, 1001-1004.
- Heidel, A.J., Clarke, J.D., Antonovics, J., and Dong, X. (2004). Fitness costs of mutations affecting the systemic acquired resistance pathway in Arabidopsis thaliana. Genetics 168, 2197-2206.
- Heil, M., and Baldwin, I.T. (2002). Fitness costs of induced resistance: emerging experimental support for a slippery concept. Trends in Plant Science 7, 61-67.
- Heinrich, M., Hettenhausen, C., Lange, T., Wünsche, H., Fang, J., Baldwin, I.T., and Wu, J. (2013). High levels of jasmonic acid antagonize the biosynthesis of gibberellins and inhibit the growth of Nicotiana attenuata stems. The Plant Journal 73, 591-606.
- Hulsen, T. (2022). DeepVenn -- a web application for the creation of area-proportional Venn diagrams using the deep learning framework Tensorflow.js. arXiv, 2210.04597v04591.
 - **Hunter**, **P.** (2022). Understanding redundancy and resilience. EMBO reports **23**, e54742.
- Huot, B., Yao, J., Montgomery, B.L., and He, S.Y. (2014). Growth–defense tradeoffs in plants: A balancing act to optimize fitness. Molecular Plant 7, 1267-1287.
- Ibañez, C., Poeschl, Y., Peterson, T., Bellstädt, J., Denk, K., Gogol-Döring, A., Quint, M., and Delker, C. (2017). Ambient temperature and genotype differentially affect

- developmental and phenotypic plasticity in Arabidopsis thaliana. BMC Plant Biology **17**, 114.
- Ishiga, Y., Ishiga, T., Uppalapati, S.R., and Mysore, K.S. (2011). Arabidopsis seedling floodinoculation technique: a rapid and reliable assay for studying plant-bacterial interactions. Plant Methods 7, 32.
- Jacobs, T.B., LaFayette, P.R., Schmitz, R.J., and Parrott, W.A. (2015). Targeted genome modifications in soybean with CRISPR/Cas9. BMC Biotechnology 15, 16.
- Jibran, R., A. Hunter, D., and P. Dijkwel, P. (2013). Hormonal regulation of leaf senescence through integration of developmental and stress signals. Plant Molecular Biology 82, 547-561.
- Jorgensen, R.A., Cluster, P.D., English, J., Que, Q., and Napoli, C.A. (1996). Chalcone synthase cosuppression phenotypes in petunia flowers: comparison of sense vs. antisense constructs and single-copy vs. complex T-DNA sequences. Plant Mol Biol 31, 957-973.

866

867

868

869

873

874

875

876

877

878

879

880

881

882

883

884

885

886

887

888

889

890

- **Kafri, R., Springer, M., and Pilpel, Y.** (2009). Genetic redundancy: New tricks for old genes. Cell **136**, 389-392.
- **Kim, J., Kim, J.H., Lyu, J.I., Woo, H.R., and Lim, P.O.** (2017). New insights into the regulation of leaf senescence in *Arabidopsis*. Journal of Experimental Botany **69,** 787-799.
- Kim, J.Y., Song, J.T., and Seo, H.S. (2021). Ammonium-mediated reduction in salicylic acid content and recovery of plant growth in Arabidopsis siz1 mutants is modulated by NDR1 and NPR1. Plant Signal Behav 16, 1928819.
 - Kim, S.H., Gao, F., Bhattacharjee, S., Adiasor, J.A., Nam, J.C., and Gassmann, W. (2010). The Arabidopsis resistance-like gene SNC1 is activated by mutations in SRFR1 and contributes to resistance to the bacterial effector AvrRps4. PLOS Pathogens 6, e1001172.
 - Kim, S.H., Son, G.H., Bhattacharjee, S., Kim, H.J., Nam, J.C., Nguyen, P.D., Hong, J.C., and Gassmann, W. (2014). The Arabidopsis immune adaptor SRFR1 interacts with TCP transcription factors that redundantly contribute to effector-triggered immunity. Plant Journal 78, 978-989.
 - Kim, Y., Park, S., Gilmour, S.J., and Thomashow, M.F. (2013). Roles of CAMTA transcription factors and salicylic acid in configuring the low-temperature transcriptome and freezing tolerance of *Arabidopsis*. Plant Journal **75**, 364-376.
 - **Kim, Y.S., Lee, M., Lee, J.H., Lee, H.J., and Park, C.M.** (2015). The unified ICE-CBF pathway provides a transcriptional feedback control of freezing tolerance during cold acclimation in *Arabidopsis*. Plant Mol Biol **89,** 187-201.
 - **Kliebenstein, D.J.** (2016). False idolatry of the mythical growth versus immunity tradeoff in molecular systems plant pathology. Physiological and Molecular Plant Pathology **95**, 55-59.
 - **Köhler, C., Merkle, T., and Neuhaus, G.** (1999). Characterisation of a novel gene family of putative cyclic nucleotide- and calmodulin-regulated ion channels in Arabidopsis thaliana. Plant J **18,** 97-104.
- Koncz, C., and Schell, J. (1986). The promoter of TL-DNA gene 5 controls the tissue-specific expression of chimaeric genes carried by a novel type of *Agrobacterium* binary vector. Molecular and General Genetics **204**, 383-396.
- Kong, X., Luo, X., Qu, G.-P., Liu, P., and Jin, J.B. (2017). Arabidopsis SUMO protease ASP1 positively regulates flowering time partially through regulating FLC stability Journal of Integrative Plant Biology **59**, 15-29.

- Korves, T.M., and Bergelson, J. (2003). A developmental response to pathogen infection in Arabidopsis. Plant Physiol **133**, 339-347.
- Kovacs, D., Kalmar, E., Torok, Z., and Tompa, P. (2008). Chaperone activity of ERD10 and ERD14, two disordered stress-related plant proteins. Plant Physiology **147**, 381-390.
- Kurkela, S., and Franck, M. (1990). Cloning and characterization of a cold-and ABA-inducible Arabidopsis gene. Plant Molecular Biology 15, 137-144.
- Kurkela, S., and Borg-Franck, M. (1992). Structure and expression of kin2, one of two coldand ABA-induced genes of Arabidopsis thaliana. Plant Molecular Biology 19, 689-692.
- Kwon, S.I., Koczan, J.M., and Gassmann, W. (2004). Two *Arabidopsis srfr* (suppressor of rps4-RLD) mutants exhibit avrRps4-specific disease resistance independent of RPS4.
 Plant Journal 40, 366-375.
- Lee, J., Nam, J., Park, H.C., Na, G., Miura, K., Jin, J.B., Yoo, C.Y., Baek, D., Kim, D.H.,
 Jeong, J.C., Kim, D., Lee, S.Y., Salt, D.E., Mengiste, T., Gong, Q., Ma, S., Bohnert,
 H.J., Kwak, S.-S., Bressan, R.A., Hasegawa, P.M., and Yun, D.-J. (2007). Salicylic
 acid-mediated innate immunity in Arabidopsis is regulated by SIZ1 SUMO E3 ligase.
 Plant Journal 49, 79-90.
- Li, S., He, L., Yang, Y., Zhang, Y., Han, X., Hu, Y., and Jiang, Y. (2024). INDUCER OF CBF EXPRESSION 1 promotes cold-enhanced immunity by directly activating salicylic acid signaling. Plant Cell https://doi.org/10.1093/plcell/koae096.
- Li, X., Svedin, E., Mo, H., Atwell, S., Dilkes, B.P., and Chapple, C. (2014). Exploiting natural variation of secondary metabolism identifies a gene controlling the glycosylation diversity of dihydroxybenzoic acids in Arabidopsis thaliana. Genetics **198**, 1267-1276.
- Li, Y., Li, S., Bi, D., Cheng, Y.T., Li, X., and Zhang, Y. (2010). SRFR1 negatively regulates plant NB-LRR resistance protein accumulation to prevent autoimmunity. PLoS Pathog 6, e1001111.
- Li, Z., Liu, H., Ding, Z., Yan, J., Yu, H., Pan, R., Hu, J., Guan, Y., and Hua, J. (2020). Low temperature enhances plant immunity via salicylic acid pathway genes that are repressed by ethylene1. Plant Physiology **182**, 626-639.
- Liao, Y., Smyth, G.K., and Shi, W. (2014). featureCounts: an efficient general purpose program for assigning sequence reads to genomic features. Bioinformatics **30**, 923-930.
- Liu, J., Qiu, G., Liu, C., Li, H., Chen, X., Fu, Q., Lin, Y., and Guo, B. (2022). Salicylic acid, a multifaceted hormone, combats abiotic stresses in plants. Life (Basel) 12.
- Liu, Q., Kasuga, M., Sakuma, Y., Abe, H., Miura, S., Yamaguchi-Shinozaki, K., and
 Shinozaki, K. (1998). Two transcription factors, DREB1 and DREB2, with an
 EREBP/AP2 DNA binding domain separate two cellular signal transduction pathways in
 drought- and low-temperature-responsive gene expression, respectively, in *Arabidopsis*.
 Plant cell 10, 1391-1406.
- Love, M., Huber, W., and Anders, S. (2014). Moderated estimation of fold change and dispersion for RNA-seq data with DESeq2. Genome Biology 15, 550.
- Lovelace, A.H., Smith, A., and Kvitko, B.H. (2018). Pattern-triggered immunity alters the transcriptional regulation of virulence-associated genes and induces the sulfur starvation response in *Pseudomonas syringae* pv. tomato DC3000. Molecular Plant-Microbe Interactions® **31**, 750-765.
- Lyons, J.M. (1973). Chilling injury in plants. Annual Review of Plant Physiology 24, 445-466.
- Ma, W., Smigel, A., Walker, R.K., Moeder, W., Yoshioka, K., and Berkowitz, G.A. (2010).

 Leaf senescence signaling: The Ca2+-conducting Arabidopsis cyclic nucleotide gated

- channel2 acts through nitric oxide to repress senescence programming. Plant Physiology **154**, 733-743.
- Machado, R.A.R., Baldwin, I.T., and Erb, M. (2017). Herbivory-induced jasmonates constrain plant sugar accumulation and growth by antagonizing gibberellin signaling and not by promoting secondary metabolite production. New Phytologist **215**, 803-812.
 - Mauch, F., Mauch-Mani, B., Gaille, C., Kull, B., Haas, D., and Reimmann, C. (2001). Manipulation of salicylate content in Arabidopsis thaliana by the expression of an engineered bacterial salicylate synthase. Plant Journal 25, 67-77.

- Miller, M., Song, Q., Shi, X., Juenger, T.E., and Chen, Z.J. (2015). Natural variation in timing of stress-responsive gene expression predicts heterosis in intraspecific hybrids of Arabidopsis. Nature Communications 6, 7453.
- Miura, K., and Tada, Y. (2014). Regulation of water, salinity, and cold stress responses by salicylic acid. Frontiers in Plant Science 5.
- Miura, K., Okamoto, H., Okuma, E., Shiba, H., Kamada, H., Hasegawa, P.M., and Murata, Y. (2013). SIZ1 deficiency causes reduced stomatal aperture and enhanced drought tolerance via controlling salicylic acid-induced accumulation of reactive oxygen species in Arabidopsis. Plant Journal 73, 91-104.
- Morris, K., Mackerness, S.A.H., Page, T., John, C.F., Murphy, A.M., Carr, J.P., and Buchanan-Wollaston, V. (2000). Salicylic acid has a role in regulating gene expression during leaf senescence. Plant Journal 23, 677-685.
- Murat, F., Louis, A., Maumus, F., Armero, A., Cooke, R., Quesneville, H., Crollius, H.R., and Salse, J. (2015). Understanding Brassicaceae evolution through ancestral genome reconstruction. Genome Biology 16, 262.
- Navarro-Retamal, C., Bremer, A., Alzate-Morales, J., Caballero, J., Hincha, D.K., Gonzalez, W., and Thalhammer, A. (2016). Molecular dynamics simulations and CD spectroscopy reveal hydration-induced unfolding of the intrinsically disordered LEA proteins COR15A and COR15B from Arabidopsis thaliana. Physical Chemistry Chemical Physics 18, 25806-25816.
- **Novillo, F., Medina, J., and Salinas, J.** (2007). *Arabidopsis* CBF1 and CBF3 have a different function than CBF2 in cold acclimation and define different gene classes in the CBF regulon. Proceedings of the National Academy of Sciences **104**, 21002-21007.
- Park, B.S., Song, J.T., and Seo, H.S. (2011). Arabidopsis nitrate reductase activity is stimulated by the E3 SUMO ligase AtSIZ1. Nat Commun 2, 400.
- Peng, S., Guo, D., Guo, Y., Zhao, H., Mei, J., Han, Y., Guan, R., Wang, T., Song, T., Sun, K., Liu, Y., Mao, T., Chang, H., Xue, J., Cai, Y., Chen, D., and Wang, S. (2022). CONSTITUTIVE EXPRESSER OF PATHOGENESIS-RELATED GENES 5 is an RNA-binding protein controlling plant immunity via an RNA processing complex. The Plant Cell 34, 1724-1744.
- **Peng, Y., Yang, J., Li, X., and Zhang, Y.** (2021). Salicylic acid: Biosynthesis and signaling. Annual Review of Plant Biology **72**, 761-791.
- Reuber, T.L., Plotnikova, J.M., Dewdney, J., Rogers, E.E., Wood, W., and Ausubel, F.M. (1998). Correlation of defense gene induction defects with powdery mildew susceptibility in Arabidopsis enhanced disease susceptibility mutants. The Plant Journal 16, 473-485.
- Rivas-San Vicente, M., and Plasencia, J. (2011). Salicylic acid beyond defence: its role in plant growth and development. Journal of Experimental Botany **62**, 3321-3338.

- 989 Scott, I.M., Clarke, S.M., Wood, J.E., and Mur, L.A.J. (2004). Salicylate accumulation 990 inhibits growth at chilling temperature in Arabidopsis. Plant Physiology 135, 1040-1049.
- Stelling, J., Sauer, U., Szallasi, Z., Doyle, F.J., and Doyle, J. (2004). Robustness of cellular 991 992 functions. Cell 118, 675-685.
- Swamy, P.S., Hu, H., Pattathil, S., Maloney, V.J., Xiao, H., Xue, L.-J., Chung, J.-D., 993 Johnson, V.E., Zhu, Y., Peter, G.F., Hahn, M.G., Mansfield, S.D., Harding, S.A., 994 995 and Tsai, C.-J. (2015). Tubulin perturbation leads to unexpected cell wall modifications 996 and affects stomatal behaviour in Populus. Journal of Experimental Botany 66, 6507-997 6518.
- 998 Tang, K., Zhao, L., Ren, Y., Yang, S., Zhu, J.-K., and Zhao, C. (2020). The transcription factor ICE1 functions in cold stress response by binding to the promoters of CBF and 999 COR genes. Journal of Integrative Plant Biology 62, 258-263. 1000

1002

1003 1004

1005

1006

1007

1008

1009

- Thalhammer, A., and Hincha, D.K. (2014). A mechanistic model of COR15 protein function in plant freezing tolerance: integration of structural and functional characteristics. Plant Signaling & Behavior 9, e977722.
- Thalhammer, A., Bryant, G., Sulpice, R., and Hincha, D.K. (2014). Disordered Cold Regulated 15 proteins protect chloroplast membranes during freezing through binding and folding, but do not stabilize chloroplast enzymes in vivo. Plant Physiology 166, 190-201.
- **Thomashow, M.F.** (1999). Plant cold acclimation: Freezing tolerance genes and regulatory mechanisms. Annual Review of Plant Physiology and Plant Molecular Biology 50, 571-599.
- Tran, S., Ison, M., Ferreira Dias, N.C., Ortega, M.A., Chen, Y.-F.S., Peper, A., Hu, L., Xu, 1010 D., Mozaffari, K., Severns, P.M., Yao, Y., Tsai, C.-J., Teixeira, P.J.P.L., and Yang, 1011 L. (2023). Endogenous salicylic acid suppresses de novo root regeneration from leaf 1012 explants. PLOS Genetics 19, e1010636. 1013
- 1014 Uknes, S., Mauch-Mani, B., Moyer, M., Potter, S., Williams, S., Dincher, S., Chandler, D., Slusarenko, A., Ward, E., and Ryals, J. (1992). Acquired resistance in *Arabidopsis*. 1015 1016 Plant Cell 4, 645-656.
- 1017 Ullah, C., Chen, Y.-H., Ortega, M.A., and Tsai, C.-J. (2023). The diversity of salicylic acid biosynthesis and defense signaling in plants: Knowledge gaps and future opportunities. 1018 Current Opinion in Plant Biology 72, 102349. 1019
- Ullah, C., Schmidt, A., Reichelt, M., Tsai, C.-J., and Gershenzon, J. (2022). Lack of 1020 antagonism between salicylic acid and jasmonate signalling pathways in poplar. New Phytologist 235, 701-717. 1022
- 1023 van Wersch, R., Li, X., and Zhang, Y. (2016). Mighty dwarfs: Arabidopsis autoimmune mutants and their usages in genetic dissection of plant immunity. Front Plant Sci 7, 1717. 1024
- Verberne, M.C., Verpoorte, R., Bol, J.F., Mercado-Blanco, J., and Linthorst, H.J.M. 1025 1026 (2000). Overproduction of salicylic acid in plants by bacterial transgenes enhances pathogen resistance. Nat Biotechnol 18, 779-783. 1027
- Vlot, A.C., Dempsey, D.M.A., and Klessig, D.F. (2009). Salicylic acid, a multifaceted hormone 1028 to combat disease. Annual Review of Phytopathology 47, 177-206. 1029
- Walters, D.R., Ratsep, J., and Havis, N.D. (2013). Controlling crop diseases using induced 1030 resistance: challenges for the future. Journal of Experimental Botany 64, 1263-1280. 1031
- Wang, D., Amornsiripanitch, N., and Dong, X. (2006). A genomic approach to identify 1032 1033 regulatory nodes in the transcriptional network of systemic acquired resistance in plants. PLOS Pathogens 2, e123. 1034

- Wang, Y., and Hua, J. (2009). A moderate decrease in temperature induces COR15a expression through the CBF signaling cascade and enhances freezing tolerance. Plant J 60, 340-349.
- Wang, Y., Bao, Z., Zhu, Y., and Hua, J. (2009). Analysis of temperature modulation of plant defense against biotrophic microbes. Molecular Plant-Microbe Interactions 22, 498-506.
- Wilhelm, K., and Thomashow, M. (1993). Arabidopsis thaliana cor15b, an apparent homologue of cor15a, is strongly responsive to cold and ABA, but not drought. Plant Molecular Biology 23, 1073-1077.
- Wu, Z., Han, S., Zhou, H., Tuang, Z.K., Wang, Y., Jin, Y., Shi, H., and Yang, W. (2019).

 Cold stress activates disease resistance in Arabidopsis thaliana through a salicylic acid dependent pathway. Plant, Cell & Environment 42, 2645-2663.

- Xue, L.-J., Alabady, M.S., Mohebbi, M., and Tsai, C.-J. (2015). Exploiting genome variation to improve next-generation sequencing data analysis and genome editing efficiency in Populus tremula x alba 717-1B4. Tree Genetics & Genomes 11, 82.
- Xue, L.-J., Guo, W., Yuan, Y., Anino, E.O., Nyamdari, B., Wilson, M.C., Frost, C.J., Chen, H.-Y., Babst, B.A., Harding, S.A., and Tsai, C.-J. (2013). Constitutively elevated salicylic acid levels alter photosynthesis and oxidative state, but not growth in transgenic *Populus*. Plant Cell **25**, 2714-2730.
- Yamaguchi-Shinozaki, K., and Shinozaki, K. (1993). Characterization of the expression of a desiccation-responsive rd29 gene of *Arabidopsis thaliana* and analysis of its promoter in transgenic plants. Molecular and General Genetics MGG **236**, 331-340.
- Yang, D.-L., Yao, J., Mei, C.-S., Tong, X.-H., Zeng, L.-J., Li, Q., Xiao, L.-T., Sun, T.-p., Li, J., Deng, X.-W., Lee, C.M., Thomashow, M.F., Yang, Y., He, Z., and He, S.Y. (2012). Plant hormone jasmonate prioritizes defense over growth by interfering with gibberellin signaling cascade. Proceedings of the National Academy of Sciences 109, E1192-E1200.
- Yang, S.-D., Seo, P.J., Yoon, H.-K., and Park, C.-M. (2011). The Arabidopsis NAC transcription factor VNI2 integrates abscisic acid signals into leaf senescence via the COR/RD genes. Plant Cell 23, 2155-2168.
- Yu, I.c., Parker, J., and Bent, A.F. (1998). Gene-for-gene disease resistance without the hypersensitive response in Arabidopsis dnd1 mutant. Proceedings of the National Academy of Sciences 95, 7819-7824.
- Yuan, M., Ngou, B.P.M., Ding, P., and Xin, X.-F. (2021). PTI-ETI crosstalk: an integrative view of plant immunity. Current Opinion in Plant Biology 62, 102030.
- Zhang, K., Halitschke, R., Yin, C., Liu, C.-J., and Gan, S.-S. (2013). Salicylic acid 3-hydroxylase regulates Arabidopsis leaf longevity by mediating salicylic acid catabolism. Proceedings of the National Academy of Sciences 110, 14807-14812.
- **Zhang, N., Zhou, S., Yang, D., and Fan, Z.** (2020). Revealing shared and distinct genes responding to JA and SA signaling in Arabidopsis by meta-analysis. Frontiers in Plant Science 11.
- Zhang, Y., Zhao, L., Zhao, J., Li, Y., Wang, J., Guo, R., Gan, S., Liu, C.-J., and Zhang, K.
 (2017). S5H/DMR6 encodes a salicylic acid 5-hydroxylase that fine-tunes salicylic acid homeostasis. Plant Physiology 175, 1082.

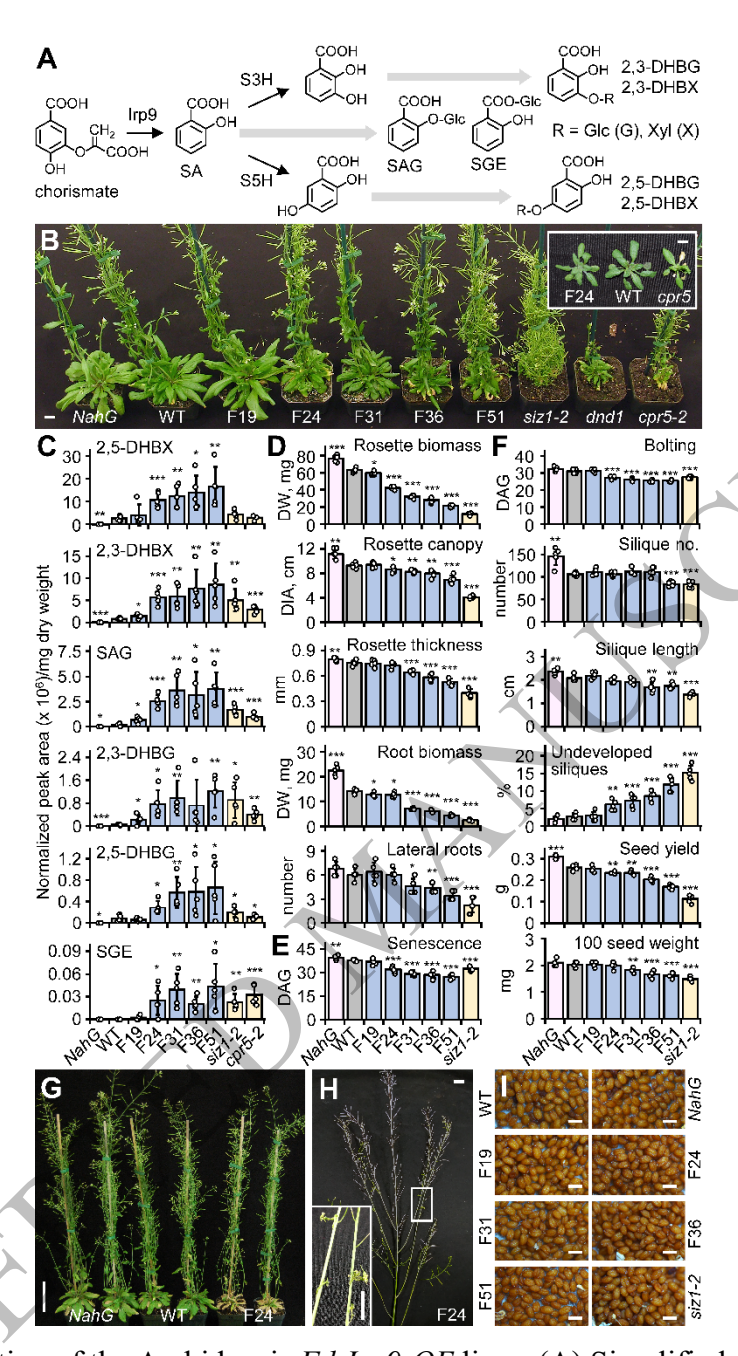


Fig. 1. Characterization of the Arabidopsis Fd-Irp9-OE lines. (A) Simplified diagram of Irp9-mediated SA biosynthesis and downstream catabolism and conjugation. (B) Representative plant morphology 45 days after germination (DAG) at 22°C. Inset shows juvenile senescence of cpr5-2 not seen in F24. Scale bars, 1 cm. (C) Levels of SA-derived conjugates in rosette leaves of wild type (WT), homozygous Fd-Irp9-OE lines, and autoimmune mutants at bolting. Data are means \pm SD of n = 5 independent pools, each sampled from three rosette leaves per plant. (D–F) Vegetative growth traits at 28 DAG (D), onset of senescence (E) and bolting (F) and seed traits at 50 DAG (F). Data are means \pm SD of n = 5 plants. (G) Premature senescence in F24 (right)

compared with WT (middle) and NahG (left). Scale bars, 5 cm. (H) Representative images of F24 at seed set (scale bar, 1 cm). Inset shows incompletely developed siliques (scale bar, 0.5 cm). (I) Representative images of seeds. Scale bars, 0.5 mm. Data are means \pm SD of n = 5 plants. Statistical significance was determined by two-sided Student's t-test against WT (***P < 0.001; **P < 0.01; **P < 0.05). The growth phenotypes were reproducible in more than 10 experiments. The experiment for SA analysis was conducted four times with similar trends. DHBG, dihydroxybenzoate glucoside; DHBX, dihydroxybenzoate xyloside; SA, salicylic acid; S3H, SA 3-hydroxylase; S5H, SA 5-hydroxylase; SAG, SA glucoside; SGE, SA glucose ester.

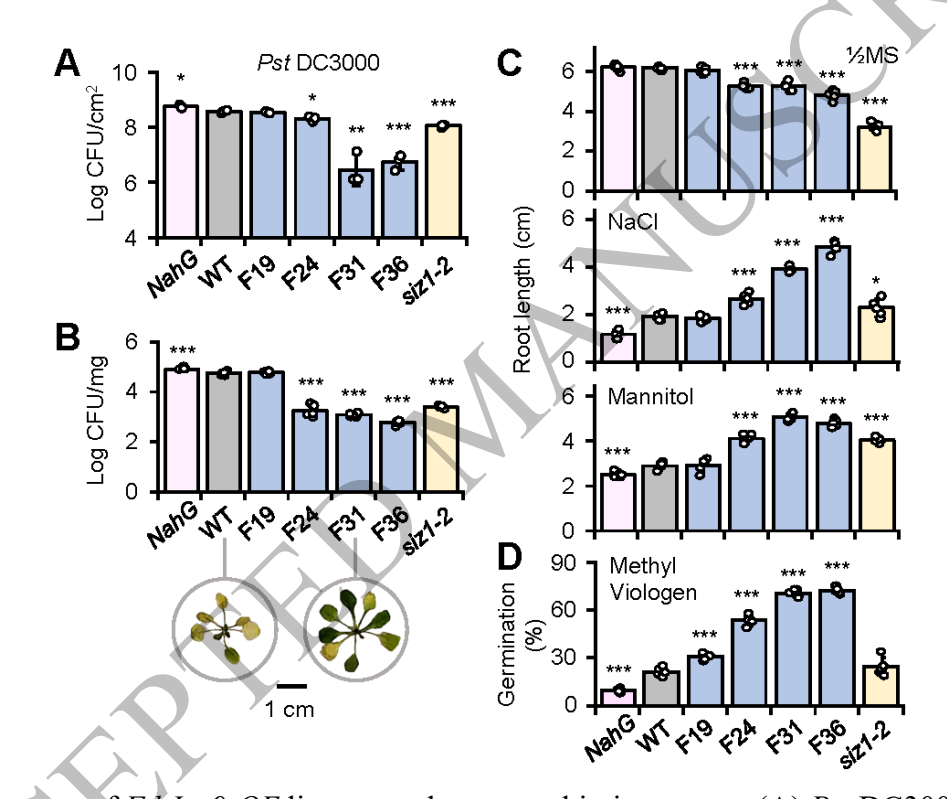


Fig. 2. Responses of Fd-Irp9-OE lines to pathogen or abiotic stresses. (A) Pst DC3000 bacterial growth based on leaf infiltration of soil-grown plants at bolting. Data are means \pm SD of n = 3 independent pools of four leaf discs sampled from two rosette leaves per plant. The experiment was performed six times with similar trends. (B) Pst DC3000 bacterial growth based on flood-inoculation of 2-week-old seedlings in tissue culture. Representative plant images from WT and F31 three days after inoculation are shown. Scale bar, 1 cm. Data are means \pm SD of n = 5 independent pools of three rosette leaves per plant. The experiment was performed twice with similar patterns. (C) Primary root growth of 11-day-old seedlings on half-strength MS medium (1/2 MS) alone or with NaCl or mannitol. Data are means \pm SD of n = 5 independent pools of

two seedlings per pool (each data point was averaged from two seedlings). (D) Seed germination in the presence of methyl viologen. Data are means \pm SD of n = 5 independent pools of 10 seeds per pool. The abiotic stress experiments were performed twice with similar results. Statistical significance was determined by two-sided Student's *t*-test against WT (***P < 0.001; **P < 0.05).

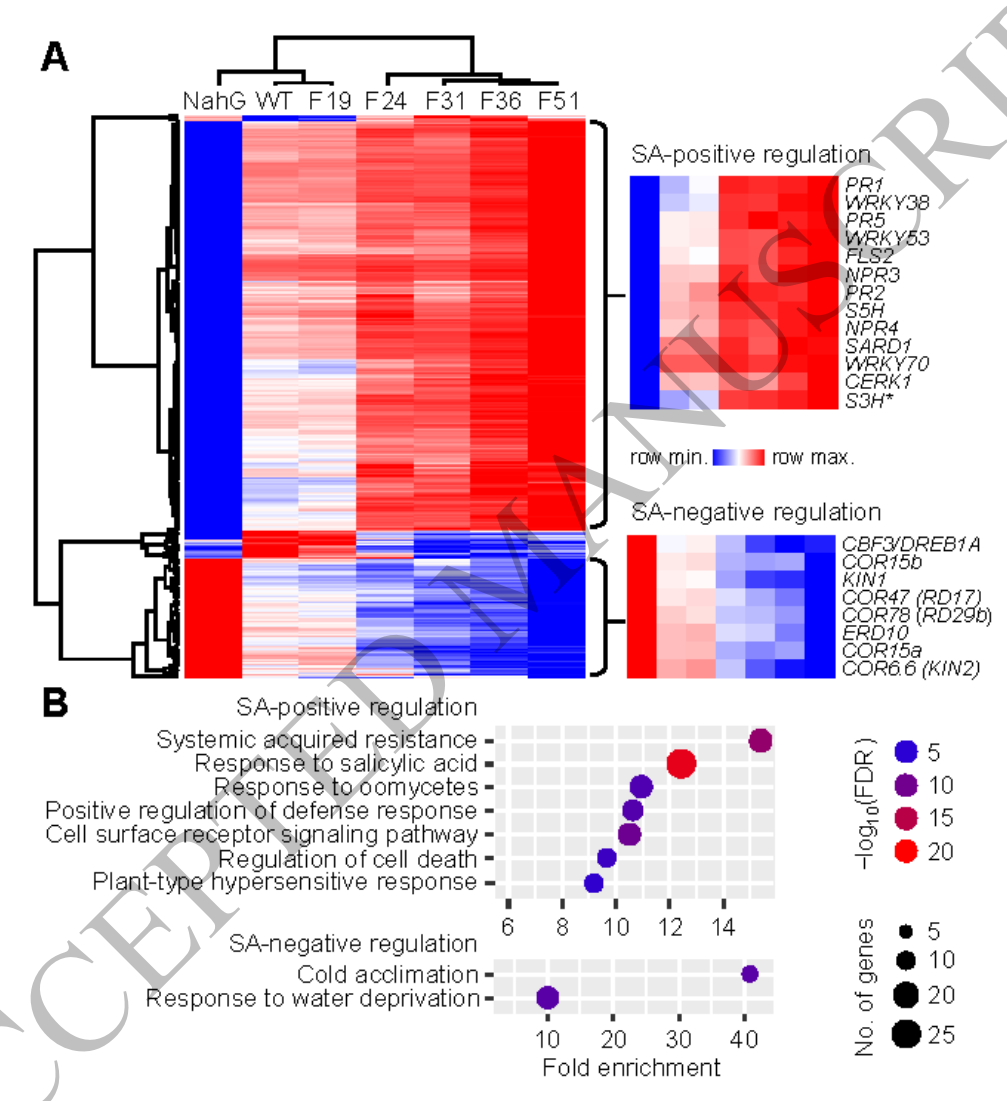


Fig. 3. Leaf transcriptomic responses of the Fd-Irp9-OE lines. (A) Hierarchical clustering of 471 SA-responsive genes selected according to differential expression in both F51 and NahG lines relative to the WT. Representative genes that were positively or negatively regulated by SA are shown on the right (*S3H not captured in the list was included for reference). Data were obtained from n = 4 independent pools, each sampled from three rosette leaves per plant at 30 DAG, except for F51 where n = 3 independent pools. Differential expression relative to WT was

determined by DEseq2 based on $Q \le 0.05$ and fold-change ≥ 1.5 . Color scale bar denotes the z-score transformed \log_2 ratios. Color scale bar denotes the normalized \log_2 ratio (B) Gene ontology (GO) enrichment of genes positively or negatively regulated by SA. Only GO terms with $-\log_{10}$ FDR > 5 and fold-enrichment > 9 are shown. The RNA-seq experiment was conducted once.

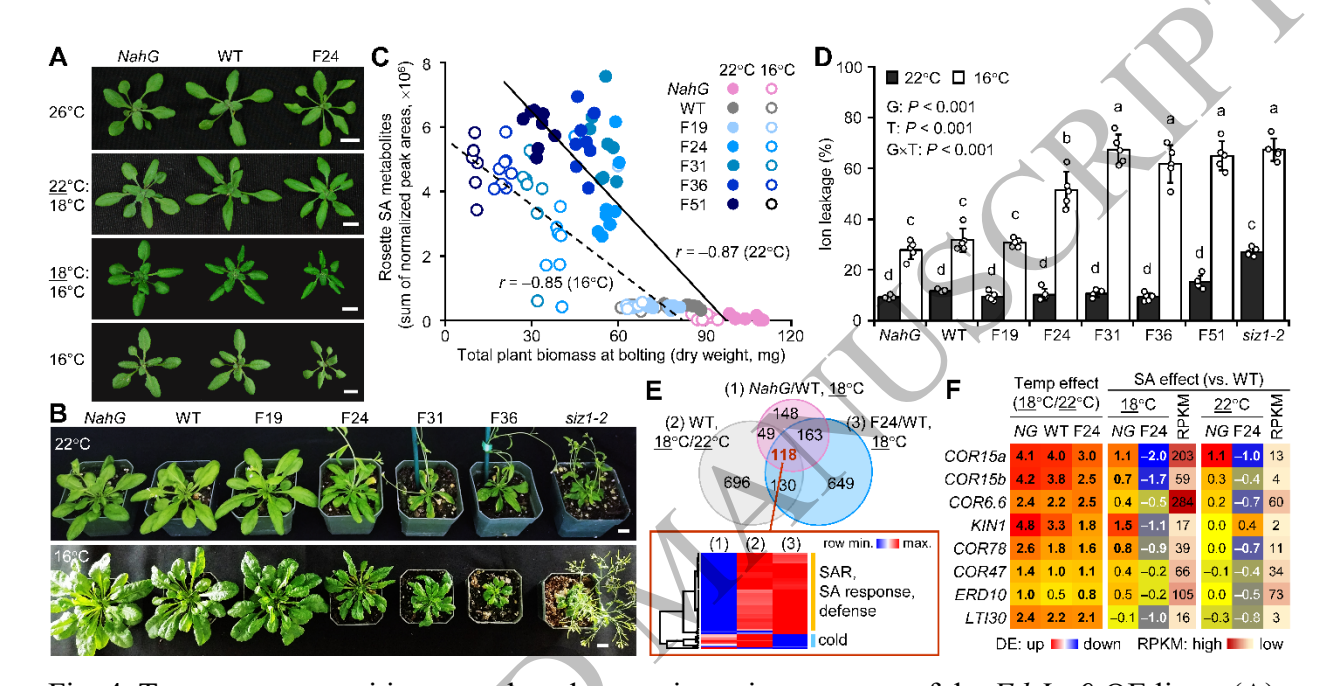


Fig. 4. Temperature-sensitive growth and transcriptomic responses of the Fd-Irp9-OE lines. (A) Representative phenotypes of NahG, WT, and F24 plants at 26°C (18 DAG), $\underline{22}$ °C:18°C (\underline{day} :night, 18 DAG), $\underline{18}$ °C:16°C (\underline{day} :night, 26 DAG), or 16°C (22 DAG). Scale bars, 1 cm. Each condition was repeated at least once with similar results. (B) Representative phenotypes of NahG, WT, Fd-Irp9-OE (low to high SA, left to right), and siz1-2 plants at 22°C (30 DAG) or 16°C (49 DAG). Scale bars, 1 cm. (C) Regression analysis between total plant biomass and total rosette SA levels of multiple genotypes grown at 22°C or 16°C (n = 8 plants except for F51 at 16°C where n = 7 plants). SA metabolite data are shown in Supplementary Figure S3A. (D) Percent ion leakage of rosette leaf 8 from plants grown at 22°C or 16°C. Data are means \pm SD (n = 5 plants). Effects of genotype (G), temperature (T), and their interaction were determined by two-way ANOVA, followed by Tukey's post-hoc tests; significance is indicated by letters. The experiments were conducted four times for growth monitoring, twice for SA measurements, and once for ion leakage analysis. (E) Venn diagram of differentially expressed genes in response to SA (NahG vs. WT or F24 vs. WT) at $\underline{18}$ °C or to temperature changes ($\underline{18}$ °C vs. $\underline{22}$ °C) in the WT.

Clustering analysis of the intersection of 118 genes is shown below, and the top GO terms are indicated on the right. Color scale bar denotes the z-score transformed \log_2 ratios. (F) Expression response heatmaps of COR genes. Values are \log_2 -transformed ratios (significant difference denoted by boldface). Average transcript abundance (reads per kilobase of transcript per million mapped reads, RPKM) of WT samples at 22° C or 18° C is also shown. Data were obtained from n=4 independent pools, each sampled from three rosette leaves per plant at bolting. Differential expression between the specified sample pair was determined by DEseq2 based on $Q \le 0.05$ and fold-change ≥ 1.5 . The RNA-seq experiment was performed once. NG, NahG.

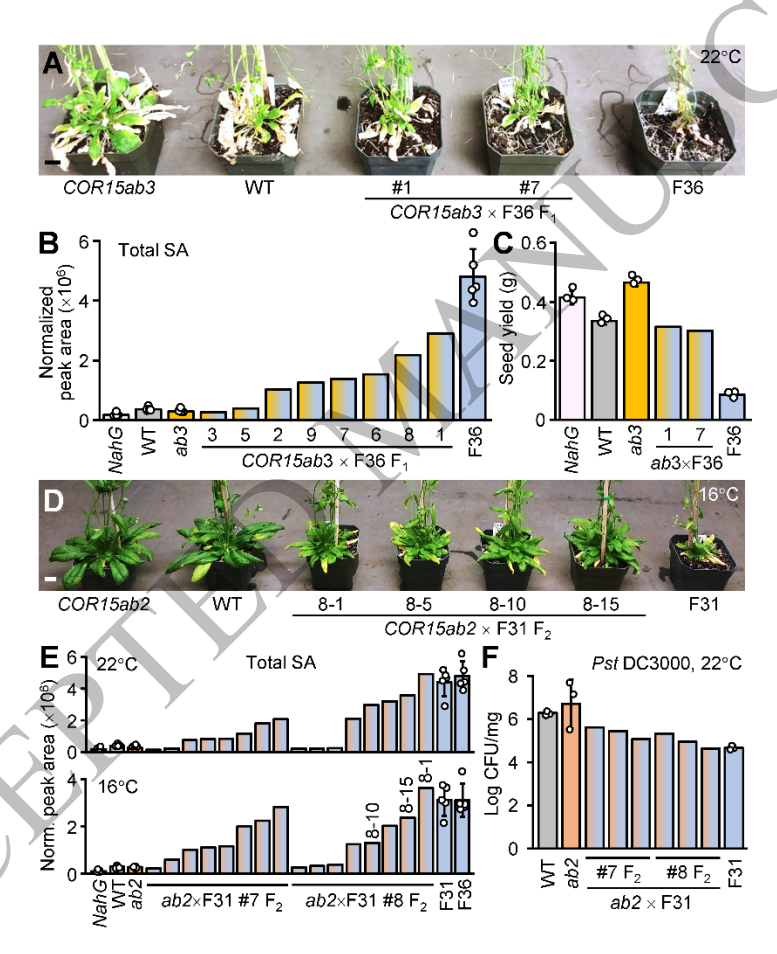
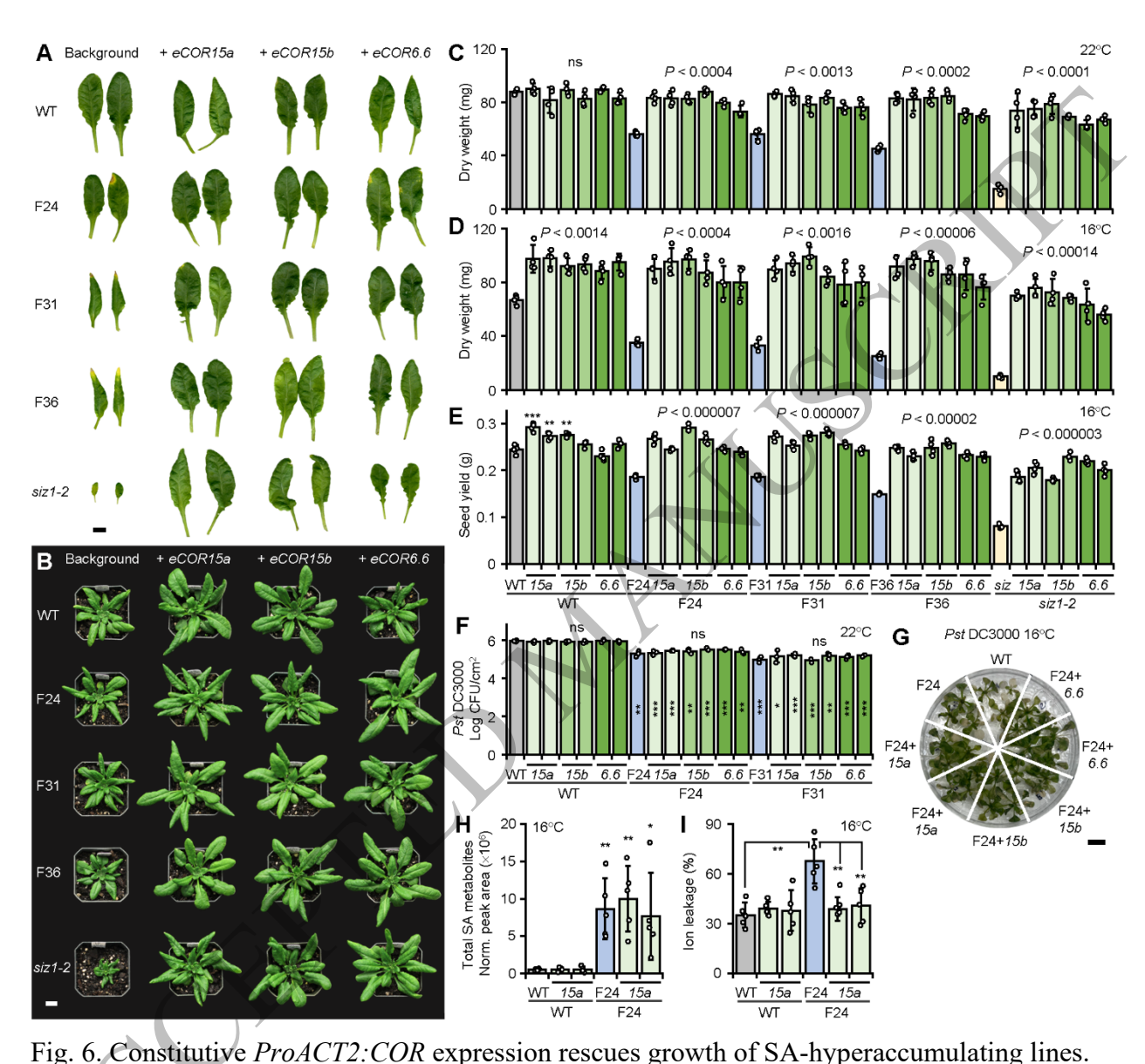


Fig. 5. F_1 and F_2 progeny phenotypes of *Pro35S:COR15ab* and hiSA crosses before the onset of silencing. (A–C) Plant growth at 65 DAG (A), total SA metabolite levels measured in leaf punches (B), and seed yield (C) of representative F_1 plants from $COR15ab3 \times F36$ at 22°C. Data for homozygous genotypes are means \pm SD of n = 5 (B) or n = 3 (C) plants. (D–F) Plant growth at 65 DAG at 16°C (D), total SA levels in leaf punches at 22°C or 16°C (E), and *Pst* DC3000 disease resistance at 22°C of representative F_2 progeny from $COR15ab2 \times F31$ F_1 #7 or #8. Data

for homozygous genotypes are means \pm SD of n = 5 (E) or n = 3 (F) plants. Each experiment was performed once. Scale bars, 1 cm.



(A) Mature leaves of representative transgenic plants expressing eCOR15a, eCOR15b, or eCOR6.6 in WT, siz1-2, and hiSA backgrounds at 22°C (30 DAG). Scale bar, 1 cm. Whole plant images are shown in Supplementary Figure S6A. (B) Plant growth of representative eCOR transgenic lines (49 DAG) at 16°C. Scale bar, 1 cm. (C–E) Rosette biomass (C–D) and seed yield (E) at 22°C (C) or 16°C (D–E) from two events per transformation (abbreviated without "eCOR"). Data are means \pm SD of n=4 plants. Statistical significance against the respective

background was determined by two-sided Student's t-test (***P < 0.001; **P < 0.01). (F) Disease resistance against Pst DC3000 based on leaf infiltration of soil-grown plants at 22°C (30 DAG). Data are means \pm SD of n = 3 independent pools, each sampled from two rosette leaves per plant per pool. No statistical significance (ns) was found against the respective background based on two-sided Student's t-test. Statistical differences against WT are indicated by asterisks inside the bar (***P < 0.001; **P < 0.01; *P < 0.05). (G) Responses to Pst DC3000 based on flood inoculation of tissue-cultured plants at 16°C. Scale bar, 1 cm. Additional replicates are shown in Supplementary Figure S6. (H–I) Total SA (H) and percent ion leakage (I) in rosettes of tissue-cultured plants at 16°C. Data are means \pm SD (n = 5 plants). Statistical significance was determined by two-sided Student's t-test against WT in (H) or as indicated (I) (**P < 0.01; *P < 0.05). The growth experiments were conducted three times with reproducible phenotypes. All other analyses were performed once.

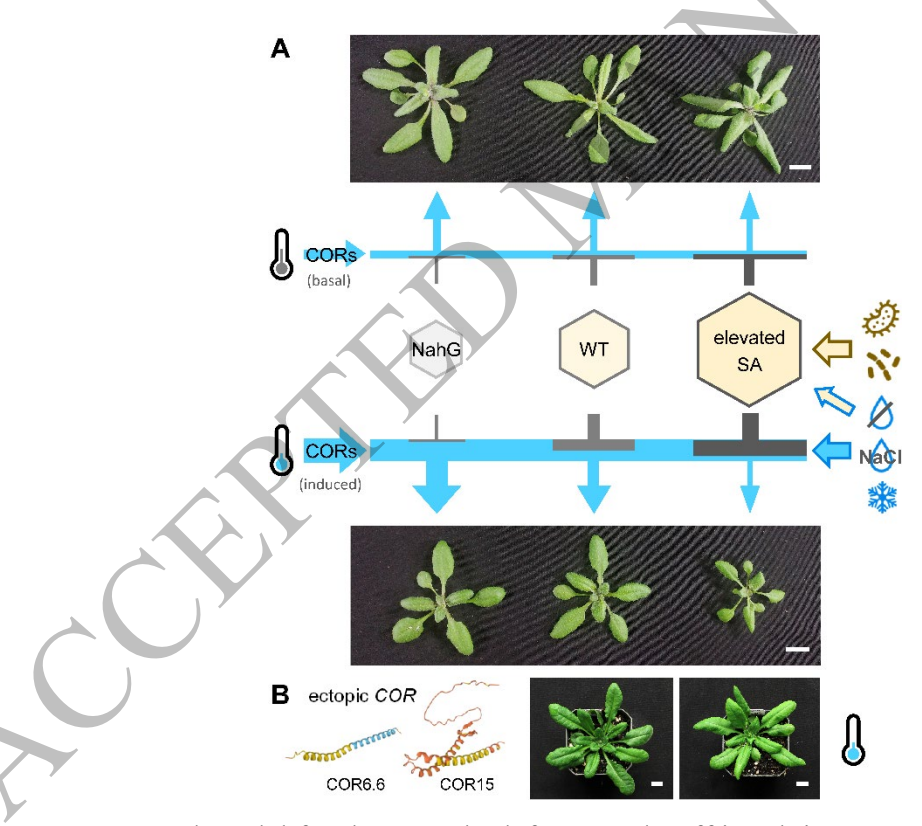


Fig. 7. A proposed model for the growth–defense trade-off involving SA and CORs in response to various stressors. (A) Plant growth under ambient conditions with basal or low levels of *COR* expression (blue arrows) is negatively affected by SA (top). CORs are strongly stimulated for membrane protection at below-ambient temperatures. This induction is attenuated by SA (grey

flatheads), resulting in exacerbated growth reduction in hiSA plants (bottom). The negative regulation of *CORs* by SA may also affect growth–defense trade-offs in response to various biotic and abiotic stressors denoted by brown and blue arrows, respectively, on the right. (B) Ectopic expression of individual *COR* genes can bypass SA suppression and rescue plant growth. Scale bars, 1 cm. The COR6.6 and COR15a structural predictions were retrieved from AlphaFold DB (https://alphafold.ebi.ac.uk).

Parsed Citations

Abreu, M.E., and Munné-Bosch, S. (2009). Salicylic acid deficiency in NahG transgenic lines and sid2 mutants increases seed yield in the annual plant Arabidopsis thaliana. Journal of Experimental Botany 60, 1261-1271.

Google Scholar: Author Only Title Only Author and Title

Aerts, N., Pereira Mendes, M., and Van Wees, S.C.M. (2021). Multiple levels of crosstalk in hormone networks regulating plant defense. Plant J 105, 489-504.

Google Scholar: Author Only Title Only Author and Title

Albrecht, T., and Argueso, C.T. (2017). Should I fight or should I grow now? The role of cytokinins in plant growth and immunity and in the growth–defence trade-off. Annals of Botany 119, 725-735.

Google Scholar: Author Only Title Only Author and Title

Alcázar, R., and Parker, J.E. (2011). The impact of temperature on balancing immune responsiveness and growth in Arabidopsis. Trends in Plant Science 16, 666-675.

Google Scholar: Author Only Title Only Author and Title

Andersson, J.M., Pham, Q.D., Mateos, H., Eriksson, S., Harryson, P., and Sparr, E. (2020). The plant dehydrin Lti30 stabilizes lipid lamellar structures in varying hydration conditions [S]. J Lipid Res 61, 1014-1024.

Google Scholar: Author Only Title Only Author and Title

Bartsch, M., Bednarek, P., Vivancos, P.D., Schneider, B., von Roepenack-Lahaye, E., Foyer, C.H., Kombrink, E., Scheel, D., and Parker, J.E. (2010). Accumulation of isochorismate-derived 2,3-dihydroxybenzoic 3-O-beta-D-xyloside in Arabidopsis resistance to pathogens and ageing of leaves. Journal of Biological Chemistry 285, 25654-25665.

Google Scholar: Author Only Title Only Author and Title

Bechtold, U., Ferguson, J.N., and Mullineaux, P.M. (2018). To defend or to grow lessons from Arabidopsis C24. Journal of Experimental Botany 69, 2809-2821.

Google Scholar: Author Only Title Only Author and Title

Bhattacharjee, S., Halane, M.K., Kim, S.H., and Gassmann, W. (2011). Pathogen effectors target Arabidopsis EDS1 and alter its interactions with immune regulators. Science 334, 1405-1408.

Google Scholar: Author Only Title Only Author and Title

Bowling, S.A, Clarke, J.D., Liu, Y., Klessig, D.F., and Dong, X. (1997). The cpr5 mutant of Arabidopsis expresses both NPR1-dependent and NPR1-independent resistance. Plant Cell 9.

Google Scholar: <u>Author Only Title Only Author and Title</u>

Boyes, D.C., Zayed, AM., Ascenzi, R., McCaskill, AJ., Hoffman, N.E., Davis, K.R., and Görlach, J. (2001). Growth stage-based phenotypic analysis of Arabidopsis: A model for high throughput functional genomics in plants. Plant Cell 13, 1499-1510.

Google Scholar: Author Only Title Only Author and Title

Browse, J., and Xin, Z. (2001). Temperature sensing and cold acclimation. Current Opinion in Plant Biology 4, 241-246. Google Scholar: Author Only Title Only Author and Title

Bruessow, F., Bautor, J., Hoffmann, G., Yildiz, I., Zeier, J., and Parker, J.E. (2021). Natural variation in temperature-modulated immunity uncovers transcription factor bHLH059 as a thermoresponsive regulator in Arabidopsis thaliana. PLOS Genetics 17, e1009290.

Google Scholar: Author Only Title Only Author and Title

Bruggeman, Q., Raynaud, C., Benhamed, M., and Delarue, M. (2015). To die or not to die? Lessons from lesion mimic mutants. Front Plant Sci 6, 24.

Google Scholar: <u>Author Only Title Only Author and Title</u>

Campos, M.L., Yoshida, Y., Major, I.T., de Oliveira Ferreira, D., Weraduwage, S.M., Froehlich, J.E., Johnson, B.F., Kramer, D.M., Jander, G., Sharkey, T.D., and Howe, G.A (2016). Rewiring of jasmonate and phytochrome B signalling uncouples plant growth-defense tradeoffs. Nat Commun 7, 12570.

Google Scholar: Author Only Title Only Author and Title

Carstens, M., McCrindle, T.K., Adams, N., Diener, A, Guzha, D.T., Murray, S.L., Parker, J.E., Denby, K.J., and Ingle, R.A (2014). Increased resistance to biotrophic pathogens in the Arabidopsis constitutive induced resistance 1 mutant is EDS1 and PAD4-dependent and modulated by environmental temperature. PLoS One 9, e109853.

Google Scholar: Author Only Title Only Author and Title

Chan, C.W., Schorrak, L.M., Smith, R.K., Jr., Bent, AF., and Sussman, M.R. (2003). A cyclic nucleotide-gated ion channel, CNGC2, is crucial for plant development and adaptation to calcium stress. Plant Physiol 132, 728-731.

Google Scholar: Author Only Title Only Author and Title

Clough, S.J., and Bent, AF. (1998). Floral dip: a simplified method for Agrobacterium -mediated transformation of Arabidopsis

thaliana. The Plant Journal 16, 735-743.

Google Scholar: Author Only Title Only Author and Title

Clough, S.J., Fengler, K.A, Yu, I.c., Lippok, B., Smith, R.K., and Bent, A.F. (2000). The Arabidopsis dnd1 "defense, no death" gene encodes a mutated cyclic nucleotide-gated ion channel. Proc Natl Acad Sci U S A 97, 9323-9328.

Google Scholar: Author Only Title Only Author and Title

Dean, J.V., and Delaney, S.P. (2008). Metabolism of salicylic acid in wild-type, ugt74f1 and ugt74f2 glucosyltransferase mutants of Arabidopsis thaliana. Physiologia Plantarum 132, 417-425.

Google Scholar: Author Only Title Only Author and Title

Ding, Y., Shi, Y., and Yang, S. (2019). Advances and challenges in uncovering cold tolerance regulatory mechanisms in plants. New Phytologist 222, 1690-1704.

Google Scholar: Author Only Title Only Author and Title

Ding, Y., Sun, T., Ao, K., Peng, Y., Zhang, Y., Li, X., and Zhang, Y. (2018). Opposite roles of salicylic acid receptors NPR1 and NPR3/NPR4 in transcriptional regulation of plant immunity. Cell 173, 1454-1467.e1415.

Google Scholar: Author Only Title Only Author and Title

Dobin, A, and Gingeras, T.R. (2015). Mapping RNA-seq reads with STAR. Curr Protoc Bioinformatics 51, 11.14.11-11.14.19. Google Scholar: Author Only Title Only Author and Title

Eriksson, S.K., Kutzer, M., Procek, J., Gröbner, G., and Harryson, P. (2011). Tunable membrane binding of the intrinsically disordered dehydrin Lti30, a cold-induced plant stress protein. Plant Cell 23, 2391-2404.

Google Scholar: Author Only Title Only Author and Title

Freh, M., Gao, J., Petersen, M., and Panstruga, R. (2022). Plant autoimmunity-fresh insights into an old phenomenon. Plant Physiology 188, 1419-1434.

Google Scholar: Author Only Title Only Author and Title

Ge, S.X., Jung, D., and Yao, R. (2020). ShinyGO: a graphical gene-set enrichment tool for animals and plants. Bioinformatics 36, 2628-2629.

Google Scholar: Author Only Title Only Author and Title

Gilmour, S.J., Hajela, R.K., and Thomashow, M.F. (1988). Cold acclimation in Arabidopsis thaliana. Plant Physiol 87, 745-750. Google Scholar: Author Only Title Only Author and Title

Gilmour, S.J., Lin, C., and Thomashow, M.F. (1996). Purification and properties of Arabidopsis thaliana COR (cold-regulated) gene polypeptides COR15am and COR6.6 expressed in Escherichia coli. Plant Physiology 111, 293-299.

Google Scholar: <u>Author Only Title Only Author and Title</u>

Gu, Y., Zebell, S.G., Liang, Z., Wang, S., Kang, B.-H., and Dong, X. (2016). Nuclear pore permeabilization is a convergent signaling event in effector-triggered immunity. Cell 166, 1526-1538.e1511.

Google Scholar: Author Only Title Only Author and Title

Hajela, R.K., Horvath, D.P., Gilmour, S.J., and Thomashow, M.F. (1990). Molecular cloning and expression of COR (Cold-Regulated) genes in Arabidopsis thaliana. Plant Physiology 93, 1246-1252.

Google Scholar: Author Only Title Only Author and Title

Hartman, J.L., Garvik, B., and Hartwell, L. (2001). Principles for the buffering of genetic variation. Science 291, 1001-1004.

Google Scholar: Author Only Title Only Author and Title

Heidel, AJ., Clarke, J.D., Antonovics, J., and Dong, X. (2004). Fitness costs of mutations affecting the systemic acquired resistance pathway in Arabidopsis thaliana. Genetics 168, 2197-2206.

Google Scholar: Author Only Title Only Author and Title

Heil, M., and Baldwin, I.T. (2002). Fitness costs of induced resistance: emerging experimental support for a slippery concept. Trends in Plant Science 7, 61-67.

Google Scholar: Author Only Title Only Author and Title

Heinrich, M., Hettenhausen, C., Lange, T., Wünsche, H., Fang, J., Baldwin, I.T., and Wu, J. (2013). High levels of jasmonic acid antagonize the biosynthesis of gibberellins and inhibit the growth of Nicotiana attenuata stems. The Plant Journal 73, 591-606. Google Scholar: Author Only Title Only Author and Title

Hulsen, T. (2022). DeepVenn -- a web application for the creation of area-proportional Venn diagrams using the deep learning framework Tensorflow.js. arXiv, 2210.04597v04591.

Google Scholar: Author Only Title Only Author and Title

Hunter, P. (2022). Understanding redundancy and resilience. EMBO reports 23, e54742.

Google Scholar: Author Only Title Only Author and Title

Huot, B., Yao, J., Montgomery, B.L., and He, S.Y. (2014). Growth–defense tradeoffs in plants: Abalancing act to optimize fitness. Molecular Plant 7, 1267-1287.

Google Scholar: Author Only Title Only Author and Title

Ibañez, C., Poeschl, Y., Peterson, T., Bellstädt, J., Denk, K., Gogol-Döring, A., Quint, M., and Delker, C. (2017). Ambient temperature and genotype differentially affect developmental and phenotypic plasticity in Arabidopsis thaliana. BMC Plant Biology 17, 114.

Google Scholar: Author Only Title Only Author and Title

Ishiga, Y., Ishiga, T., Uppalapati, S.R., and Mysore, K.S. (2011). Arabidopsis seedling flood-inoculation technique: a rapid and reliable assay for studying plant-bacterial interactions. Plant Methods 7, 32.

Google Scholar: Author Only Title Only Author and Title

Jacobs, T.B., LaFayette, P.R., Schmitz, R.J., and Parrott, W.A. (2015). Targeted genome modifications in soybean with CRISPR/Cas9. BMC Biotechnology 15, 16.

Google Scholar: Author Only Title Only Author and Title

Jibran, R., A Hunter, D., and P. Dijkwel, P. (2013). Hormonal regulation of leaf senescence through integration of developmental and stress signals. Plant Molecular Biology 82, 547-561.

Google Scholar: Author Only Title Only Author and Title

Jorgensen, R.A., Cluster, P.D., English, J., Que, Q., and Napoli, C.A. (1996). Chalcone synthase cosuppression phenotypes in petunia flowers: comparison of sense vs. antisense constructs and single-copy vs. complex T-DNA sequences. Plant Mol Biol 31, 957-973.

Google Scholar: Author Only Title Only Author and Title

Kafri, R., Springer, M., and Pilpel, Y. (2009). Genetic redundancy: New tricks for old genes. Cell 136, 389-392.

Google Scholar: Author Only Title Only Author and Title

Kim, J., Kim, J.H., Lyu, J.I., Woo, H.R., and Lim, P.O. (2017). New insights into the regulation of leaf senescence in Arabidopsis. Journal of Experimental Botany 69, 787-799.

Google Scholar: Author Only Title Only Author and Title

Kim, J.Y., Song, J.T., and Seo, H.S. (2021). Ammonium-mediated reduction in salicylic acid content and recovery of plant growth in Arabidopsis siz1 mutants is modulated by NDR1 and NPR1. Plant Signal Behav 16, 1928819.

Google Scholar: Author Only Title Only Author and Title

Kim, S.H., Gao, F., Bhattacharjee, S., Adiasor, J.A, Nam, J.C., and Gassmann, W. (2010). The Arabidopsis resistance-like gene SNC1 is activated by mutations in SRFR1 and contributes to resistance to the bacterial effector AvrRps4. PLOS Pathogens 6, e1001172.

Google Scholar: Author Only Title Only Author and Title

Kim, S.H., Son, G.H., Bhattacharjee, S., Kim, H.J., Nam, J.C., Nguyen, P.D., Hong, J.C., and Gassmann, W. (2014). The Arabidopsis immune adaptor SRFR1 interacts with TCP transcription factors that redundantly contribute to effector-triggered immunity. Plant Journal 78, 978-989.

Google Scholar: Author Only Title Only Author and Title

Kim, Y., Park, S., Gilmour, S.J., and Thomashow, M.F. (2013). Roles of CAMTA transcription factors and salicylic acid in configuring the low-temperature transcriptome and freezing tolerance of Arabidopsis. Plant Journal 75, 364-376.

Google Scholar: Author Only Title Only Author and Title

Kim, Y.S., Lee, M., Lee, J.H., Lee, H.J., and Park, C.M. (2015). The unified ICE-CBF pathway provides a transcriptional feedback control of freezing tolerance during cold acclimation in Arabidopsis. Plant Mol Biol 89, 187-201.

Google Scholar: Author Only Title Only Author and Title

Kliebenstein, D.J. (2016). False idolatry of the mythical growth versus immunity tradeoff in molecular systems plant pathology. Physiological and Molecular Plant Pathology 95, 55-59.

Google Scholar: Author Only Title Only Author and Title

Köhler, C., Merkle, T., and Neuhaus, G. (1999). Characterisation of a novel gene family of putative cyclic nucleotide- and calmodulin-regulated ion channels in Arabidopsis thaliana. Plant J 18, 97-104.

Google Scholar: Author Only Title Only Author and Title

Koncz, C., and Schell, J. (1986). The promoter of TL-DNA gene 5 controls the tissue-specific expression of chimaeric genes carried by a novel type of Agrobacterium binary vector. Molecular and General Genetics 204, 383-396.

Google Scholar: Author Only Title Only Author and Title

Kong, X., Luo, X., Qu, G.-P., Liu, P., and Jin, J.B. (2017). Arabidopsis SUMO protease ASP1 positively regulates flowering time partially through regulating FLC stability Journal of Integrative Plant Biology 59, 15-29.

Google Scholar: Author Only Title Only Author and Title

Korves, T.M., and Bergelson, J. (2003). Adevelopmental response to pathogen infection in Arabidopsis. Plant Physiol 133, 339-347.

Google Scholar: Author Only Title Only Author and Title

Kovacs, D., Kalmar, E., Torok, Z., and Tompa, P. (2008). Chaperone activity of ERD10 and ERD14, two disordered stress-related plant proteins. Plant Physiology 147, 381-390.

Google Scholar: Author Only Title Only Author and Title

Kurkela, S., and Franck, M. (1990). Cloning and characterization of a cold-and ABA-inducible Arabidopsis gene. Plant Molecular Biology 15, 137-144.

Google Scholar: Author Only Title Only Author and Title

Kurkela, S., and Borg-Franck, M. (1992). Structure and expression of kin2, one of two cold- and ABA-induced genes of Arabidopsis thaliana. Plant Molecular Biology 19, 689-692.

Google Scholar: Author Only Title Only Author and Title

Kwon, S.I., Koczan, J.M., and Gassmann, W. (2004). Two Arabidopsis srfr (suppressor of rps4-RLD) mutants exhibit avrRps4-specific disease resistance independent of RPS4. Plant Journal 40, 366-375.

Google Scholar: <u>Author Only Title Only Author and Title</u>

Lee, J., Nam, J., Park, H.C., Na, G., Miura, K., Jin, J.B., Yoo, C.Y., Baek, D., Kim, D.H., Jeong, J.C., Kim, D., Lee, S.Y., Salt, D.E., Mengiste, T., Gong, Q., Ma, S., Bohnert, H.J., Kwak, S.-S., Bressan, R.A, Hasegawa, P.M., and Yun, D.-J. (2007). Salicylic acid-mediated innate immunity in Arabidopsis is regulated by SIZ1 SUMO E3 ligase. Plant Journal 49, 79-90.

Google Scholar: <u>Author Only Title Only Author and Title</u>

Li, S., He, L., Yang, Y., Zhang, Y., Han, X., Hu, Y., and Jiang, Y. (2024). INDUCER OF CBF EXPRESSION 1 promotes cold-enhanced immunity by directly activating salicylic acid signaling. Plant Cell https://doi.org/10.1093/plcell/koae096.

Google Scholar: Author Only Title Only Author and Title

Li, X., Svedin, E., Mo, H., Atwell, S., Dilkes, B.P., and Chapple, C. (2014). Exploiting natural variation of secondary metabolism identifies a gene controlling the glycosylation diversity of dihydroxybenzoic acids in Arabidopsis thaliana. Genetics 198, 1267-1276.

Google Scholar: Author Only Title Only Author and Title

Li, Y., Li, S., Bi, D., Cheng, Y.T., Li, X., and Zhang, Y. (2010). SRFR1 negatively regulates plant NB-LRR resistance protein accumulation to prevent autoimmunity. PLoS Pathog 6, e1001111.

Google Scholar: Author Only Title Only Author and Title

Li, Z, Liu, H., Ding, Z, Yan, J., Yu, H., Pan, R., Hu, J., Guan, Y., and Hua, J. (2020). Low temperature enhances plant immunity via salicylic acid pathway genes that are repressed by ethylene1. Plant Physiology 182, 626-639.

Google Scholar: <u>Author Only Title Only Author and Title</u>

Liao, Y., Smyth, G.K., and Shi, W. (2014). featureCounts: an efficient general purpose program for assigning sequence reads to genomic features. Bioinformatics 30, 923-930.

Google Scholar: Author Only Title Only Author and Title

Liu, J., Qiu, G., Liu, C., Li, H., Chen, X., Fu, Q., Lin, Y., and Guo, B. (2022). Salicylic acid, a multifaceted hormone, combats abiotic stresses in plants. Life (Basel) 12.

Google Scholar: Author Only Title Only Author and Title

Liu, Q., Kasuga, M., Sakuma, Y., Abe, H., Miura, S., Yamaguchi-Shinozaki, K., and Shinozaki, K. (1998). Two transcription factors, DREB1 and DREB2, with an EREBP/AP2 DNA binding domain separate two cellular signal transduction pathways in drought- and low-temperature-responsive gene expression, respectively, in Arabidopsis. Plant cell 10, 1391-1406.

Google Scholar: Author Only Title Only Author and Title

Love, M., Huber, W., and Anders, S. (2014). Moderated estimation of fold change and dispersion for RNA-seq data with DESeq2. Genome Biology 15, 550.

Google Scholar: <u>Author Only Title Only Author and Title</u>

Lovelace, A.H., Smith, A, and Kvitko, B.H. (2018). Pattern-triggered immunity alters the transcriptional regulation of virulence-associated genes and induces the sulfur starvation response in Pseudomonas syringae pv. tomato DC3000. Molecular Plant-Microbe Interactions® 31, 750-765.

Google Scholar: Author Only Title Only Author and Title

Lyons, J.M. (1973). Chilling injury in plants. Annual Review of Plant Physiology 24, 445-466.

Google Scholar: Author Only Title Only Author and Title

Ma, W., Smigel, A, Walker, R.K., Moeder, W., Yoshioka, K., and Berkowitz, G.A (2010). Leaf senescence signaling: The Ca2+conducting Arabidopsis cyclic nucleotide gated channel2 acts through nitric oxide to repress senescence programming. Plant Physiology 154, 733-743.

Machado, R.A.R., Baldwin, I.T., and Erb, M. (2017). Herbivory-induced jasmonates constrain plant sugar accumulation and growth by antagonizing gibberellin signaling and not by promoting secondary metabolite production. New Phytologist 215, 803-812.

Google Scholar: Author Only Title Only Author and Title

Mauch, F., Mauch-Mani, B., Gaille, C., Kull, B., Haas, D., and Reimmann, C. (2001). Manipulation of salicylate content in Arabidopsis thaliana by the expression of an engineered bacterial salicylate synthase. Plant Journal 25, 67-77.

Google Scholar: Author Only Title Only Author and Title

Miller, M., Song, Q., Shi, X., Juenger, T.E., and Chen, Z.J. (2015). Natural variation in timing of stress-responsive gene expression predicts heterosis in intraspecific hybrids of Arabidopsis. Nature Communications 6, 7453.

Google Scholar: Author Only Title Only Author and Title

Miura, K., and Tada, Y. (2014). Regulation of water, salinity, and cold stress responses by salicylic acid. Frontiers in Plant Science

Google Scholar: Author Only Title Only Author and Title

Miura, K., Okamoto, H., Okuma, E., Shiba, H., Kamada, H., Hasegawa, P.M., and Murata, Y. (2013). SIZ1 deficiency causes reduced stomatal aperture and enhanced drought tolerance via controlling salicylic acid-induced accumulation of reactive oxygen species in Arabidopsis. Plant Journal 73, 91-104.

Google Scholar: Author Only Title Only Author and Title

Morris, K., Mackerness, S.A.H., Page, T., John, C.F., Murphy, A.M., Carr, J.P., and Buchanan-Wollaston, V. (2000). Salicylic acid has a role in regulating gene expression during leaf senescence. Plant Journal 23, 677-685.

Google Scholar: Author Only Title Only Author and Title

Murat, F., Louis, A., Maumus, F., Armero, A., Cooke, R., Quesneville, H., Crollius, H.R., and Salse, J. (2015). Understanding Brassicaceae evolution through ancestral genome reconstruction, Genome Biology 16, 262.

Google Scholar: Author Only Title Only Author and Title

Navarro-Retamal, C., Bremer, A., Azate-Morales, J., Caballero, J., Hincha, D.K., Gonzalez, W., and Thalhammer, A (2016). Molecular dynamics simulations and CD spectroscopy reveal hydration-induced unfolding of the intrinsically disordered LEA proteins COR15A and COR15B from Arabidopsis thaliana. Physical Chemistry Chemical Physics 18, 25806-25816.

Google Scholar: Author Only Title Only Author and Title

Novillo, F., Medina, J., and Salinas, J. (2007). Arabidopsis CBF1 and CBF3 have a different function than CBF2 in cold acclimation and define different gene classes in the CBF regulon. Proceedings of the National Academy of Sciences 104, 21002-21007.

Google Scholar: Author Only Title Only Author and Title

Park, B.S., Song, J.T., and Seo, H.S. (2011). Arabidopsis nitrate reductase activity is stimulated by the E3 SUMO ligase AtSIZ1. Nat Commun 2, 400.

Google Scholar: Author Only Title Only Author and Title

Peng, S., Guo, D., Guo, Y., Zhao, H., Mei, J., Han, Y., Guan, R., Wang, T., Song, T., Sun, K., Liu, Y., Mao, T., Chang, H., Xue, J., Cai, Y., Chen, D., and Wang, S. (2022). CONSTITUTIVE EXPRESSER OF PATHOGENESIS-RELATED GENES 5 is an RNA-binding protein controlling plant immunity via an RNA processing complex. The Plant Cell 34, 1724-1744.

Google Scholar: Author Only Title Only Author and Title

Peng, Y., Yang, J., Li, X., and Zhang, Y. (2021). Salicylic acid: Biosynthesis and signaling. Annual Review of Plant Biology 72, 761-791.

Google Scholar: Author Only Title Only Author and Title

Reuber, T.L., Plotnikova, J.M., Dewdney, J., Rogers, E.E., Wood, W., and Ausubel, F.M. (1998). Correlation of defense gene induction defects with powdery mildew susceptibility in Arabidopsis enhanced disease susceptibility mutants. The Plant Journal 16, 473-485.

Google Scholar: Author Only Title Only Author and Title

Rivas-San Vicente, M., and Plasencia, J. (2011). Salicylic acid beyond defence: its role in plant growth and development. Journal of Experimental Botany 62, 3321-3338.

Google Scholar: Author Only Title Only Author and Title

Scott, I.M., Clarke, S.M., Wood, J.E., and Mur, L.AJ. (2004). Salicylate accumulation inhibits growth at chilling temperature in Arabidopsis. Plant Physiology 135, 1040-1049.

Google Scholar: Author Only Title Only Author and Title

Stelling, J., Sauer, U., Szallasi, Z., Doyle, F.J., and Doyle, J. (2004). Robustness of cellular functions. Cell 118, 675-685. Google Scholar: Author Only Title Only Author and Title

Swamy, P.S., Hu, H., Pattathil, S., Maloney, V.J., Xiao, H., Xue, L.-J., Chung, J.-D., Johnson, V.E., Zhu, Y., Peter, G.F., Hahn, M.G., Mansfield, S.D., Harding, S.A., and Tsai, C.-J. (2015). Tubulin perturbation leads to unexpected cell wall modifications and affects stomatal behaviour in Populus. Journal of Experimental Botany 66, 6507-6518.

Google Scholar: Author Only Title Only Author and Title

Tang, K., Zhao, L., Ren, Y., Yang, S., Zhu, J.-K., and Zhao, C. (2020). The transcription factor ICE1 functions in cold stress response by binding to the promoters of CBF and COR genes. Journal of Integrative Plant Biology 62, 258-263.

Google Scholar: Author Only Title Only Author and Title

Thalhammer, A, and Hincha, D.K. (2014). Amechanistic model of COR15 protein function in plant freezing tolerance: integration of structural and functional characteristics. Plant Signaling & Behavior 9, e977722.

Google Scholar: Author Only Title Only Author and Title

Thalhammer, A, Bryant, G., Sulpice, R., and Hincha, D.K. (2014). Disordered Cold Regulated15 proteins protect chloroplast membranes during freezing through binding and folding, but do not stabilize chloroplast enzymes in vivo. Plant Physiology 166, 190-201.

Google Scholar: Author Only Title Only Author and Title

Thomashow, M.F. (1999). Plant cold acclimation: Freezing tolerance genes and regulatory mechanisms. Annual Review of Plant Physiology and Plant Molecular Biology 50, 571-599.

Google Scholar: Author Only Title Only Author and Title

Tran, S., Ison, M., Ferreira Dias, N.C., Ortega, M.A., Chen, Y.-F.S., Peper, A., Hu, L., Xu, D., Mozaffari, K., Severns, P.M., Yao, Y., Tsai, C.-J., Teixeira, P.J.P.L., and Yang, L. (2023). Endogenous salicylic acid suppresses de novo root regeneration from leaf explants. PLOS Genetics 19, e1010636.

Google Scholar: Author Only Title Only Author and Title

Uknes, S., Mauch-Mani, B., Moyer, M., Potter, S., Williams, S., Dincher, S., Chandler, D., Slusarenko, A, Ward, E., and Ryals, J. (1992). Acquired resistance in Arabidopsis. Plant Cell 4, 645-656.

Google Scholar: Author Only Title Only Author and Title

Ullah, C., Chen, Y.-H., Ortega, M.A, and Tsai, C.-J. (2023). The diversity of salicylic acid biosynthesis and defense signaling in plants: Knowledge gaps and future opportunities. Current Opinion in Plant Biology 72, 102349.

Google Scholar: Author Only Title Only Author and Title

Ullah, C., Schmidt, A, Reichelt, M., Tsai, C.-J., and Gershenzon, J. (2022). Lack of antagonism between salicylic acid and jasmonate signalling pathways in poplar. New Phytologist 235, 701-717.

Google Scholar: <u>Author Only</u> <u>Title Only</u> <u>Author and Title</u>

van Wersch, R., Li, X., and Zhang, Y. (2016). Mighty dwarfs: Arabidopsis autoimmune mutants and their usages in genetic dissection of plant immunity. Front Plant Sci 7, 1717.

Google Scholar: Author Only Title Only Author and Title

Verberne, M.C., Verpoorte, R., Bol, J.F., Mercado-Blanco, J., and Linthorst, H.J.M. (2000). Overproduction of salicylic acid in plants by bacterial transgenes enhances pathogen resistance. Nat Biotechnol 18, 779-783.

Google Scholar: Author Only Title Only Author and Title

Vlot, A.C., Dempsey, D.M.A, and Klessig, D.F. (2009). Salicylic acid, a multifaceted hormone to combat disease. Annual Review of Phytopathology 47, 177-206.

Google Scholar: Author Only Title Only Author and Title

Walters, D.R., Ratsep, J., and Havis, N.D. (2013). Controlling crop diseases using induced resistance: challenges for the future. Journal of Experimental Botany 64, 1263-1280.

Google Scholar: <u>Author Only Title Only Author and Title</u>

Wang, D., Amornsiripanitch, N., and Dong, X. (2006). A genomic approach to identify regulatory nodes in the transcriptional network of systemic acquired resistance in plants. PLOS Pathogens 2, e123.

Google Scholar: Author Only Title Only Author and Title

Wang, Y., and Hua, J. (2009). A moderate decrease in temperature induces COR15a expression through the CBF signaling cascade and enhances freezing tolerance. Plant J 60, 340-349.

Google Scholar: Author Only Title Only Author and Title

Wang, Y., Bao, Z., Zhu, Y., and Hua, J. (2009). Analysis of temperature modulation of plant defense against biotrophic microbes. Molecular Plant-Microbe Interactions 22, 498-506.

Google Scholar: Author Only Title Only Author and Title

Wilhelm, K., and Thomashow, M. (1993). Arabidopsis thaliana cor15b, an apparent homologue of cor15a, is strongly responsive to cold and ABA, but not drought. Plant Molecular Biology 23, 1073-1077.

Google Scholar: Author Only Title Only Author and Title

Wu, Z, Han, S., Zhou, H., Tuang, ZK., Wang, Y., Jin, Y., Shi, H., and Yang, W. (2019). Cold stress activates disease resistance in

Downloaded from https://academic.oup.com/plcell/advance-article/doi/10.1093/plcell/koae210/7721303 by guest on 31 July 2024

Arabidopsis thaliana through a salicylic acid dependent pathway. Plant, Cell & Environment 42, 2645-2663.

Google Scholar: Author Only Title Only Author and Title

Xue, L.-J., Alabady, M.S., Mohebbi, M., and Tsai, C.-J. (2015). Exploiting genome variation to improve next-generation sequencing data analysis and genome editing efficiency in Populus tremula x alba 717-1B4. Tree Genetics & Genomes 11, 82.

Google Scholar: Author Only Title Only Author and Title

Xue, L.-J., Guo, W., Yuan, Y., Anino, E.O., Nyamdari, B., Wilson, M.C., Frost, C.J., Chen, H.-Y., Babst, B.A, Harding, S.A, and Tsai, C.-J. (2013). Constitutively elevated salicylic acid levels alter photosynthesis and oxidative state, but not growth in transgenic Populus. Plant Cell 25, 2714-2730.

Google Scholar: Author Only Title Only Author and Title

Yamaguchi-Shinozaki, K., and Shinozaki, K. (1993). Characterization of the expression of a desiccation-responsive rd29 gene of Arabidopsis thaliana and analysis of its promoter in transgenic plants. Molecular and General Genetics MGG 236, 331-340.

Google Scholar: Author Only Title Only Author and Title

Yang, D.-L., Yao, J., Mei, C.-S., Tong, X.-H., Zeng, L.-J., Li, Q., Xiao, L.-T., Sun, T.-p., Li, J., Deng, X.-W., Lee, C.M., Thomashow, M.F., Yang, Y., He, Z., and He, S.Y. (2012). Plant hormone jasmonate prioritizes defense over growth by interfering with gibberellin signaling cascade. Proceedings of the National Academy of Sciences 109, E1192-E1200.

Google Scholar: Author Only Title Only Author and Title

Yang, S.-D., Seo, P.J., Yoon, H.-K., and Park, C.-M. (2011). The Arabidopsis NAC transcription factor VNI2 integrates abscisic acid signals into leaf senescence via the COR/RD genes. Plant Cell 23, 2155-2168.

Google Scholar: Author Only Title Only Author and Title

Yu, I.c., Parker, J., and Bent, AF. (1998). Gene-for-gene disease resistance without the hypersensitive response in Arabidopsis dnd1 mutant. Proceedings of the National Academy of Sciences 95, 7819-7824.

Google Scholar: Author Only Title Only Author and Title

Yuan, M., Ngou, B.P.M., Ding, P., and Xin, X.-F. (2021). PTI-ETI crosstalk: an integrative view of plant immunity. Current Opinion in Plant Biology 62, 102030.

Google Scholar: Author Only Title Only Author and Title

Zhang, K., Halitschke, R., Yin, C., Liu, C.-J., and Gan, S.-S. (2013). Salicylic acid 3-hydroxylase regulates Arabidopsis leaf longevity by mediating salicylic acid catabolism. Proceedings of the National Academy of Sciences 110, 14807-14812.

Google Scholar: Author Only Title Only Author and Title

Zhang, N., Zhou, S., Yang, D., and Fan, Z. (2020). Revealing shared and distinct genes responding to JA and SA signaling in Arabidopsis by meta-analysis. Frontiers in Plant Science 11.

Google Scholar: <u>Author Only Title Only Author and Title</u>

Zhang, Y., Zhao, L., Zhao, J., Li, Y., Wang, J., Guo, R., Gan, S., Liu, C.-J., and Zhang, K. (2017). S5H/DMR6 encodes a salicylic acid 5-hydroxylase that fine-tunes salicylic acid homeostasis. Plant Physiology 175, 1082.

Google Scholar: Author Only Title Only Author and Title

